AD-759 088

Environment Enhanced Fatigue Crack Growth in High-Strength Steels

Lehigh University

prepared for
Office of Naval Research

MARCH 1973

Distributed By:

NTIS
National Technical Information Service
U. S. DEPARTMENT OF COMMERCE

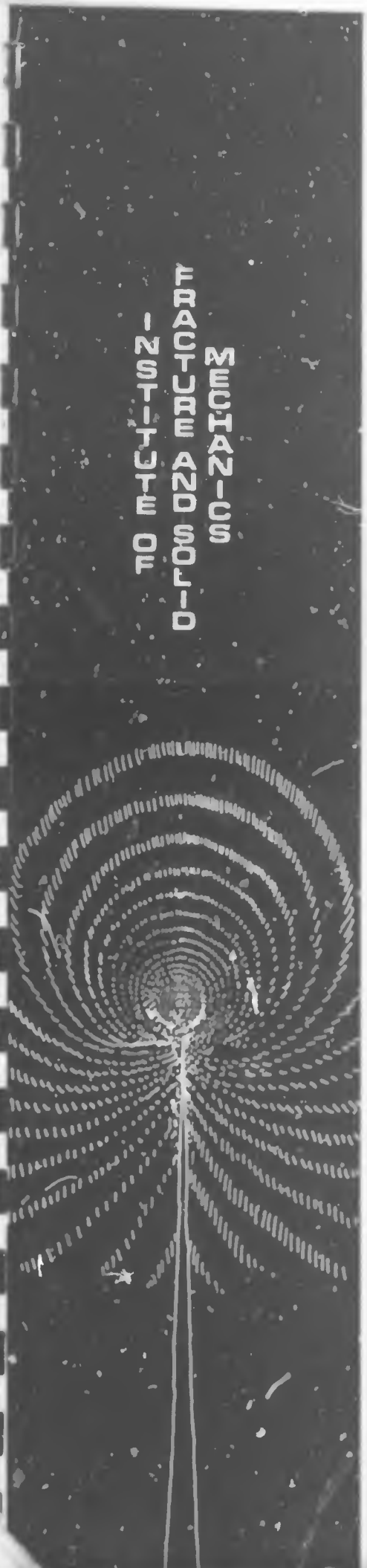

IFSM-73-39

LEHIGH UNIVERSITY

ENVIRONMENT ENHANCED FATIGUE CRACK GROWTH IN HIGH-STRENGTH STEELS

by

R. P. Wei

G. W. Simmons

March 1973

Technical Report No. 1

Office of Naval Research

Contract Nonr N00014-67-A-0370-0008, NR 036-097

Technical Report No. 1 to the Office of Naval Research
Contract Nonr N00014-67-A-0370-0008, NR 036-097

ENVIRONMENT ENHANCED FATIGUE CRACK GROWTH IN HIGH-STRENGTH STEELS

by

R. P. Wei and G. W. Simmons
LEHIGH UNIVERSITY
Bethlehem, Pennsylvania U.S.A.

Prepared for presentation at the International Conference on Stress Corrosion Cracking and Hydrogen Embrittlement of Iron Base Alloys, 42 Unieux-Firminy, France, 11-17 June 1973.

Unclassified

Security Classification

DOCUMENT CONTROL DATA - R & D

(Security classification of title, body of abstract and indexing annotation must be entered when the overall report is classified)

1. ORIGINATING ACTIVITY (Corporate author)

Institute of Fracture & Solid Mechanics
Lehigh University
Bethlehem, Pennsylvania 18015

2a. REPORT SECURITY CLASSIFICATION

Unclassified

2b. GROUP

3. REPORT TITLE

Environment Enhanced Fatigue Crack Growth in High-strength Steels

4. DESCRIPTIVE NOTES (Type of report and inclusive dates)

Technical Report No. 1 to Office of Naval Research

5. AUTHOR(S) (First name, middle initial, last name)

R. P. Wei and G. W. Simmons

6. REPORT DATE

March 1973

7a. TOTAL NO. OF PAGES

~~58~~ 61

7b. NO. OF REFS

72

8a. CONTRACT OR GRANT NO.

Nonr N00014-67-A-0370-0008

b. PROJECT NO.

NR 036-097

c.

d.

9a. ORIGINATOR'S REPORT NUMBER(S)

9b. OTHER REPORT NO(S) (Any other numbers that may be assigned this report)

10. DISTRIBUTION STATEMENT

This document has been approved for public release and sale; its distribution is unlimited.

11. SUPPLEMENTARY NOTES

12. SPONSORING MILITARY ACTIVITY

Office of Naval Research

13. ABSTRACT

The current state of understanding of the phenomenology and mechanism(s) for corrosion fatigue of high-strength steels is reviewed. Particular attention is directed towards corrosion fatigue in hydrogen and in water/water vapor environments. Since a comprehensive review of these topics was given during the 1971 International Conference on Corrosion Fatigue, this review will be restricted to a summary of the salient points and to work reported since 1971.

Available experimental data indicate that fatigue crack growth in high-strength steels is influenced by loading variables, such as frequency, stress ratio and waveform in regions above and below K_{Iscc}. The influences of these variables are directly attributed to interactions with the external chemical environment. Corrosion fatigue behavior above K_{Iscc} may be correlated with stress corrosion cracking data. Below K_{Iscc} such correlation is not possible because of the synergistic interactions between environment and fatigue crack growth. Possible synergistic interactions and their relation to chemical reaction kinetics are indicated.

Pertinent information on oxygen-metal and water-metal reactions is summarized. On the basis of the reviews, combined chemical and mechanical investigations that are needed for extending the present understanding of corrosion fatigue are considered. Initial results from a coordinated program of study for determining the water-metal reaction kinetics and the kinetics of crack growth on a single high-strength steel are discussed.

DD FORM 1 NOV 68 1473 REPLACES DD FORM 1473, 1 JAN 64, WHICH IS OBSOLETE FOR ARMY USE.

Unclassified

Security Classification

14. KEY WORDS	LINK A		LINK B		LINK C	
	ROLE	WT	ROLE	WT	ROLE	WT
Corrosion Fatigue						
High-Strength Steels						
Fracture Mechanics						
Surface Chemistry						
Chemisorption						
Loading Variables						

I. INTRODUCTION

Corrosion fatigue is a generic term that describes the response of a material to the conjoint actions of cyclic loading and corrosive (aggressive) environments. The corrosion fatigue response of a material can be measured in terms of the numbers of stress or strain cycles to produce failure, N_f, or the rate of fatigue crack growth, $\Delta a/\Delta N$, under given loading conditions. In the first case, the applied stress or strain is used as a measure of the mechanical driving force, and experimentation generally involves the use of smooth or mildly notched specimens. In the latter case, the mechanical crack driving force is characterized in terms of the crack-tip stress-intensity factor, K, defined by linear elasticity, and crack growth measurements are made on specimens that contain a single (dominant) crack. Tests of smooth or mildly notched specimens are often loosely regarded as initiation tests (even though they involve both crack initiation and growth), while tests of cracked specimens involve exclusively crack growth. Studies of corrosion fatigue have been reported as early as 1917 [1], and utilized principally the first of the two approaches. In recent years, the emphasis in studies of corrosion fatigue has been shifted to considerations of fatigue crack growth. The reasons for this shift are two-fold. First, current structural design procedures utilize fail-safe and safe-life concepts that presume the presence or early initiation of cracks in the structures, and therefore dictate considerations of crack growth. Second, because of the inability to clearly separate crack initiation from crack growth, the more traditional approach has failed to provide unambiguous information that is useful either for quantitative design or for understanding the mechanisms for corrosion fatigue. To distinguish between the two different approaches, "environment enhanced fatigue crack growth" will be used to describe specifically the crack growth aspects of corrosion fatigue here. In this paper only the crack growth aspect of the corrosion fatigue problem will be considered.

Characterization of material response and prediction of service performance of structures under corrosion fatigue conditions, unlike that for stress corrosion cracking, are complicated because of the need to incorporate the multitude of loading variables (such as mean load, cyclic-load amplitude and waveform, and frequency) and their interactions with a range of service environments. Further complications are introduced by delays in fatigue crack growth that result from complex load interactions in variable-amplitude loading and by the attendant environmental effects. The development and utilization of data on environment enhanced fatigue crack growth require a better understanding of the phenomenology and of the mechanism(s) for corrosion fatigue.

In this paper, the current state of understanding of the phenomenology and mechanism(s) of environment enhanced fatigue crack growth is reviewed. For simplicity, review of data is limited principally to hydrogen and water/water vapor environments. Data in salt or sea water are included, when appropriate. Since comprehensive reviews of the subject have been given during the International Conference on Corrosion Fatigue in 1971 [2-5], this review is limited to a summary of salient points and to work reported since 1971. Based on this review, the correlation between environment enhanced fatigue crack growth and stress corrosion cracking, and the mechanistic and surface chemistry aspects of corrosion fatigue are discussed. Combined chemical and mechanical investigations that are needed to further the understanding of environment enhanced fatigue crack growth are described and discussed.

II. PHENOMENOLOGY

Fatigue crack growth in high-strength steels, akin to that in other high-strength alloys, may be characterized in terms of the general patterns of behavior illustrated schematically in Figures 1 and 2 [2]. The rate of fatigue crack growth in an inert environment is illustrated in Figure 1. It depends strongly on K_{max}, or ΔK, at K_{max} levels approaching K_{Ic} or K_c at the high end and at levels of K_{max} or ΔK approaching an apparent threshold at the low end. In the intermediate region, the growth rate depends on some power of K_{max}, or ΔK, of the order of 2 to 10. The upper end corresponds to the onset of unstable fracturing. The lower end corresponds to some apparent limiting stress-intensity level for crack growth and appears to be related to the metallurgical structure [6-9]. K_{max}, ΔK, K_{Ic} and K_c refer to the maximum stress-intensity in a given fatigue cycle, the cyclic stress-intensity range, and the plane-strain and "thin-section" fracture toughness, respectively.

Environment enhanced fatigue crack growth response may be broadly characterized in terms of three general patterns of behavior as illustrated in Figure 2. These patterns of behavior may be discussed in relation to an apparent threshold stress intensity factor for stress corrosion cracking, K_{Iscc}* [10, 11]. The first type of behavior (hereafter referred to as Type A), represents those steel-environment systems where K_{Iscc} approaches K_{Ic}, and the environmental effects result from the synergistic actions of fatigue and corrosion [2-4, 12]. The environmental effect is evidenced by a reduction in the apparent threshold for crack growth and by increases in the rate of crack growth at given K_{max} or ΔK levels relative to that obtained in an inert environment. As K_{max}

* K_{Iscc} is the threshold K_I below which, presumably, no failure can occur as a result of stress corrosion cracking. It is very difficult to determine in practice [11]. For the purpose of this discussion, K_{Iscc} shall be defined as the asymptotic value of K_I as the rate of crack growth approaches zero.

approaches K_{Ic} or K_c, the environmental influences are diminished as a result of either the rate limiting nature of transport processes or other mechanical-chemical interactions. The second type of behavior (Type B) represents those systems where there is a substantial environment-enhanced sustained-load crack growth (stress corrosion cracking) component [2, 3, 12, 13], with K_{Iscc} substantially less than K_{Ic} or K_c. The environmental effects are quite strong above K_{Iscc} and are negligible below this level. A broad range of steel-environment (and other alloy-environment) systems would exhibit behaviors (Type C) that fall between these two extremes, with Type A behavior at K_{max} levels below the apparent threshold K (K_{Iscc}) and Type B behavior above this threshold. The overall response and types of behavior undoubtedly depend on the complex interactions between environmental, metallurgical and mechanical loading variables. Responses to specific variables can differ depending on the type of behavior pattern, and can provide insight into the possible mechanism(s) for environment-enhanced fatigue crack growth. The influences of environmental and loading variables on crack growth are most conveniently discussed in terms of the "above K_{Iscc}" (Types B and C) and "below K_{Iscc}" (Types A and C) behaviors, and are illustrated by examples.

Frequency

Cyclic load frequency is an important loading variable and can have a significant effect on fatigue crack growth. In considering the effect of frequency, however, it is necessary to distinguish between that which is "intrinsic" to the material (that is, due to rate sensitivity of the material), and that caused by interactions with the environment. Experimental evidence obtained to date suggests that there is essentially no intrinsic frequency effect for most high-strength structural alloys over a range of frequencies from 1/60 to 150 Hz, and that the observed frequency dependence is strictly related to

environmental interactions [7, 12-17].

For steel-environment systems that exhibit Types B and C behaviors, the dependence on cyclic load frequency above K_{Iscc} can be very strong, and is related to the inverse of the frequency (that is, $\Delta a/\Delta N \sim 1/f$). The effect of frequency appears to be related to the environmental sensitivity of the steel, which in turn depends on composition and microstructure (or heat treatment) [13, 15-23]. Typical examples of effect of frequency above K_{Iscc} are given by the data on a 18Ni(250) maraging steel tested in hydrogen at 1 atmosphere and room temperature, Figure 3 [13], and on an AISI 4340 steel tested in distilled water at room temperature, Figure 4 [17]. Comparison of these data with the results on sustained-load crack growth, using a superposition model suggested by Wei and Landes, indicate that the frequency dependence is directly related to the sustained-load crack growth characteristics of the alloys [13, 17]. Synergistic effect of fatigue and corrosion, if present, is usually small [13, 17]. (A more detailed review of the Wei-Landes model and its implication regarding the relationship between corrosion fatigue and stress corrosion cracking is given in Section III).

Below K_{Iscc} (that is, for Types A and C behaviors), recent experimental results suggest that some synergistic effect may be present, and that the effect may be influenced by frequency and by the waveform of the applied load, Figures 5-7 [3, 4, 16, 17]. (Discussion of the waveform effect will be deferred to a later section). The rate of environment-enhanced fatigue crack growth exhibits a maximum at some intermediate frequency depending on the steel-environment system, and approaches the growth rate in an inert environment at high frequencies and, presumably, at very low frequencies [3, 4, 16]. Comparable data on other alloy-environment systems are not available. The observed frequency dependence suggests a complex interplay involving the rate of production of fresh surfaces by fatigue, the kinetics of adsorption, the rate of repassivation,

and the rate of transport. Further fundamental studies are needed for a better understanding of frequency effects.

Stress Ratio

The rate of fatigue crack growth is affected by the stress ratio, R, in both inert and aggressive environments. Stress ratio is defined as the ratio between the minimum and the maximum values of stress-intensity (or applied stress or load) in a given cycle of loading ($R = K_{min}/K_{max}$). The effect of stress ratio on fatigue crack growth for high-strength steels has not been examined extensively. This has been caused in part by the popular notion that the stress-intensity range [$\Delta K = K_{max} - K_{min} = K_{max}(1-R)$] is the most significant variable that controls fatigue crack growth. For crack growth in an inert environment, the dependence on R is expected to be quite similar to that observed for a Ti-6Al-4V alloy tested in air, Figure 8, and for other high-strength alloys [24]. Data on an AISI 4340 steel (tempered at 200°F) generally support this observation, Figure 9 [24]. These figures show that fatigue crack growth is a function of both ΔK and R, and that stress ratio must be considered as a significant variable.

The influence of stress ratio on fatigue crack growth for $K_{max} > K_{Iscc}$ (Types B and C) is also shown in Figure 9 and in Figure 10. The increased effectiveness of the environment at the higher stress ratios is consistent with the increased amounts of time spent at K levels above K_{Iscc} in a given cycle, and is consistent with the Wei-Landes superposition model [13]. For $K_{max} < K_{Iscc}$ (Types A and C), experimental data are quite limited. Available information suggests that the fatigue crack growth response will be similar to that observed in an inert environment (see Figures 7-9, for example), and that environment enhancement appears to be essentially unaltered by changes in stress ratio [17].

Waveform

The influence of cyclic-load waveform on fatigue crack growth has begun to receive serious attention only recently [4, 17, 25, 26]. For crack growth in an inert environment at room temperature, waveform appears to have no effect over a range of frequencies from 0.1 Hz to 10 Hz [4, 17, 25, 26]. For environment-enhanced fatigue crack growth at K_{max} above K_{Iscc} (Types B and C behaviors), an effect of waveform would be expected on the basis of differences in the effective time spent at K levels above K_{Iscc}. The waveform effect is expected to be dependent on the stress ratio and on the relative value between K_{max} and K_{Iscc}. Experimental results on an AISI 4340 steel (tempered at 200°F) tested in distilled water show that there are no appreciable differences between the rates of fatigue crack growth obtained under sinusoidal, sawtooth (or triangular) and square-wave loadings at R = 0.8, Figure 11a [17]. Distinct effect was observed, however, for R = 0.1, Figure 11b [17]. The observed effects are consistent with expectations and have been discussed in detail by Miller et al. [17].

For environment-enhanced fatigue crack growth below K_{Iscc} (Types A and C behaviors), Barsom showed that waveform can have a significant and unusual effect in a 12Ni-5Cr-3Mo steel tested in salt water [4]. His results showed that waveforms that have a "slow" rise time (such as sine waves) produced full environmental effect, while waveforms with "fast" rise-times produced little or no environment enhancement of crack growth, Figure 12. These results were confirmed by Miller et al. [17] on a low-alloy steel (RQ-360A) tested in distilled water, Figure 7. No effect of waveform was observed, however, for environment-enhanced fatigue crack growth in aluminum alloys [25, 26]. Clearly the effect of waveform is peculiar to specific material-environment systems, that is, it is dependent on the particular embrittlement mechanism. Clarification of these waveform effects depends on further understanding of the chemical processes

for embrittlement. Possible experiments for the development of this understanding are considered in Section IV.

Thickness

The effect of material thickness (or more appropriately the relative thickness, defined in terms of the ratio between material thickness and some measure of the crack-tip plastic zone size) on fatigue crack growth is complicated, and has not been examined carefully for high-strength steels. Thickness can influence fatigue behavior through its effect on fracture toughness K_c, and through its effect on the apparent environment sensitivity of the material associated with a "plane-strain" to "plane-stress" fracture mode transition. The effect of thickness provides circumstantial evidence for distinguishing between a "surface" or "volume" mechanism for embrittlement, but should only be used in conjunction with other independent studies [12]. Comparisons of literature data suggest that environment sensitivity of high-strength steels in aqueous environments is not seriously altered by material thickness [21, 27].

Fracture Toughness and Metallurgical Variables

Considerations of these variables are combined because variations in metallurgical variables (such as chemical composition, heat treatment and microstructure, etc.) invariably produce changes in fracture toughness. Experimental data in this area, however, are less than conclusive. Wei et al [18] and Imhof and Barsom [28] showed that the influence of environment on fatigue crack growth is reduced in medium-carbon low-alloy high-strength steels when these steels were tempered at higher tempering temperatures (see Figure 13 for example). Increases in tempering temperature in these steels had produced both changes in the overall microstructure and improvements in fracture toughness [18, 28, 29]. Recent results by Miller et al. [17] suggest that changes in fracture toughness without an associated change in overall microstructure (for an AISI 4340 steel

tempered at 200°F and at 500°F) would not lead to improvement in the susceptibility to stress corrosion cracking or corrosion fatigue. The implication that overall microstructure is the controlling variable, however, cannot be generalized to other steels and/or environments. The results of Wei et al [18] for 18Ni(250) and 18Ni(300) maraging steels indicated definite differences in susceptibility to environment-enhanced fatigue crack growth corresponding to differences in fracture toughness, although the overall microstructures of these two steels are quite similar. The susceptibility of the maraging steels are different to that of the medium-carbon low-alloy steels at comparable strength and toughness levels. Although impurities (such as sulfur and phosphorous) can, and do affect fracture toughness, experimental results on AISI 4340 steels suggest that changes in the bulk concentration of these impurities do not appear to alter the susceptibility to environment enhanced crack growth [17, 21].

The lack of correlation between susceptibility, microstructure, and fracture toughness suggest that the processes for environment-enhanced subcritical crack growth and for unstable fracturing can be different. The preferred paths for environment-enhanced crack growth can be different from the paths for unstable fracture. Identification of the preferred paths, and examinations of the chemical composition and reactivity of these regions are essential for the understanding of environment-enhanced crack growth.

Temperature

Experimental evidence has shown that the rate of fatigue crack growth can be affected strongly by temperature [30-32]. The temperature dependence may be related to the deformation properties of the steel (for pure fatigue) or may be related to the environment-metal interaction that produces "embrittlement." Careful studies of the temperature dependence for crack growth and for appropriate chemical processes could

provide the needed insight for understanding the mechanisms for environment-enhanced fatigue crack growth, and a means for estimating the very low rates of fatigue crack growth that cannot be obtained readily and economically in normal testing. For mechanistic studies, care must be taken to separate the effects of deformation and environmental attack.

Some Further Observations on Crack Growth

In all of the previous discussions, it was implicitly assumed that there is a one-to-one correspondence between the rate of crack growth and the mechanical crack driving force (K or ΔK), under constant conditions; that is the rate of crack growth is a constant for a given K or ΔK. This is indeed the case for steady-state crack growth. The possible occurrence of nonsteady-state crack growth, however, cannot be ignored. Nonsteady-state crack growth has, in fact, been observed and reported [11, 17, 21]. Wei et al. [11] indicated that the crack growth process under sustained loading in an aggressive (corrosive) environment may be divided into five stages which depend on the magnitude of the applied stress intensity: (1) transient crack growth on loading that terminates in an incubation period, (2) incubation period during which the rate of crack growth is less than say 10^{-8} inch per second, (3) crack acceleration to a steady state condition, (4) steady-state crack growth where the rate is independent of time for a given K, and (5) unstable growth leading to rapid fracture. The incubation period and periods of crack acceleration and steady-state crack growth for two K levels are illustrated in Figure 14 [17]. Nonsteady-state crack growth can also occur in fatigue in high-strength steels, and may be seen in Figure 15 at the start of a test and following an overnight shutdown [17]. Nonsteady-state crack growth is undoubtedly associated with the process of establishing an equilibrium chemical environment in the crack-tip region, and would be intimately related to the embrittlement mechanism.

III. CORROSION FATIGUE AND STRESS CORROSION CRACKING

Recent studies have led to the suggestion of a quantitative method for estimating the effect of aggressive environments on fatigue-crack growth in some ultrahigh-strength steels at K levels above K_{Iscc} (Types B and C) [13]. This suggestion was based on an accumulation of experimental evidence and fractographic observations that indicated the mechanism for environmental enhancement of fatigue-crack growth and for crack growth under sustained loads is the same. In this method, the rate of fatigue-crack growth in an aggressive environment is considered to be the sum of the rate of fatigue-crack growth in an inert reference environment and an environmental component to be computed from the load profile and sustained-load crack growth data obtained in an identical aggressive environment.* Experimental results have shown that this superposition method correctly predicts the effects of test frequency and mean load or stress ratio, at K levels above some apparent threshold K value (K_{Iscc}) for ultrahigh-strength steels tested in gaseous hydrogen, distilled water, and water vapor environments, and for a Ti-8Al-1V-1Mo alloy tested in distilled water and in salt solution [12, 13, 15, 17, 21]. The ability to predict the rates of fatigue-crack growth in an aggressive environment for different loading conditions directly from two sets of laboratory data (that for sustained-load crack growth in the aggressive environment and that for fatigue-crack growth in an inert reference environment) is of obvious engineering significance. It would not only reduce, drastically, the amount of testing needed for material characterization, but also provide a useful basis for the development of meaningful procedures for estimating the serviceable lives

* A similar model had been suggested by McEvily and Bond [33] for corrosion fatigue of α-brass in a tarnishing solution. The sustained load component was identified with the rate of film formation which was assumed to be stress independent. In the model considered by Wei and Landes [13] no specific mechanism was postulated, and the crack velocity was taken to be dependent on K.

of engineering structures. Mechanistically, the good correlation suggests that understandings in the mechanisms for stress corrosion cracking may be transferred directly to corrosion fatigue. This superposition method, however, cannot account for the behavior below K_{Iscc} observed by Barsom [4, 16] and by Miller et al. [17]. Nevertheless, the same metal-environment interaction must be taking place at $K < K_{Iscc}$ as that at $K > K_{Iscc}$. Therefore, the mechanism for "embrittlement" is expected to be the same. The principal difference resides in the fact that fatigue is a more effective process for creating new crack surfaces than sustained loading. Careful examination of the kinetics of various chemical processes is expected to be enlightening.

Although hydrogen embrittlement or embrittlement by chloride ions has been inferred from experimental results on water- and salt-water-enhanced crack growth in high strength steels, the precise mechanism(s) have not been established. For example, studies of water-enhanced crack-growth under sustained loads in medium carbon, low-alloy ultrahigh-strength steels were carried out by Johnson and Willner [34], Hancock and Johnson [35], Hanna et al. [36], and Van der Sluys [37]. These workers suggested that the plausible mechanism for water-enhanced crack growth in these steels is hydrogen embrittlement. Wei, Talda and Li [18] suggested that oxidation per se should not be ruled out on the basis of their fatigue-crack growth studies which included two tests in a bromine vapor environment. Fractographic observations reported by Spitzig, Talda and Wei [19] showed that the paths of fracture for specimens tested in "dry" hydrogen and in moist environments are different and provide a further basis for questioning the validity of the suggested hydrogen embrittlement mechanism. Further mechanistic studies are needed to develop information for clarification of the response of materials to corrosion fatigue and will be discussed in the following section.

IV. SURFACE CHEMISTRY

The foregoing discussions indicate that the identification of mechanisms for environment-enhanced fatigue-crack growth depend, in part, on the determination of the kinetics and activation energies for the reactions of the various gases at "clean" metal surfaces produced by fatigue. Furthermore, the rates, mechanisms, and activation energies for diffusion of chemical species into the bulk need to be known. The interest in correlating surface chemistry studies with experimental observations on environment-enhanced fatigue-crack growth is exemplified by the lack of agreement on whether crack-growth kinetics in humid environments is controlled by surface reactions or by hydrogen diffusion. In this regard, it is important to note that the apparent activation energy for sustained-load crack growth of high strength steels in hydrogen is about 5 kcal/mole and is about 9 kcal/mole in water [21, 24, 37-40]. In addition, determination of the kinetics of surface chemical reactions is required for clarification of the influences of frequency and waveform on corrosion fatigue below K_{Iscc}, and for understanding various stages of nonsteady state crack growth. Because chemisorption and corrosion fatigue behavior are expected to be influenced by alloy and boundary (grain boundary) compositions, mechanical and chemical experiments will have to be conducted on the same alloys. It is beyond the scope of this paper to consider all of the specific chemical reactions that relate to mechanisms of stress corrosion or corrosion fatigue for a wide variety of steel environment systems. The surface chemistry considerations given here are, therefore, restricted to the analysis of boundary surfaces of steels, and to the reactions of water vapor with iron and high-strength steels. Because of utilization of high-strength steels in air, the discussion also includes oxygen/metal reactions and the influence of oxygen on water/metal interactions.

Chemical Composition of Boundary Surfaces

Although heat treatments are frequently used as a means of attaining homogeneity or a given microstructure in metals, it is also well known that heat treatments can lead to segregation of alloying and residual impurity elements on surfaces such as grain boundaries. A number of mechanisms for thermally induced segregation and depletion of elements near surfaces have been proposed [41-45]. The equilibrium models for segregation suggest that the enrichment of solute atoms is limited to a few atom layers from the surface. The enrichment of solute atoms over regions of few microns near the surface, on the other hand, is associated with thermally induced non-equilibrium flux of vacancies, i.e. nonequilibrium segregation. The elements that tend to segregate and the extent of segregation are complex functions of alloy composition and thermal history. Grain boundary segregation has been studied extensively because of its importance in temper embrittlement. The chemical composition of internal boundary surfaces can influence the alloy susceptibility and/or the path for environmentally enhanced fatigue crack growth. Until recently, sensitive methods have not been available for correlating specific compositions with brittle fracture, intergranular corrosion, stress corrosion, and corrosion fatigue. Auger spectroscopy is one of the available techniques for determining elemental compositions within 2 to 5 atomic layers of a surface, and has been used successfully for determining specific elements associated with temper embrittlement [46]. This technique has also been used to correlate grain-boundary composition of steels with their susceptibility to intergranular corrosion [47]. It is reasonable, therefore, to extend this technique to the characterization of surface associated with stress corrosion cracking and corrosion fatigue.

The principles of Auger spectroscopy and its applications have been detailed elsewhere and only a brief description will be given here [48-50]. Auger spectroscopy is based on the phenomenon of de-excitation of ionized atoms by the ejection of electrons as an alternative to the emission of characteristic X-rays. The energy distribution of Auger electrons is characteristic of the atoms from which they originate. The Auger electron energy spectrum can therefore be used for elemental analysis. Initial ionization of atoms in the surface is induced by an incident electron beam. Auger electrons with energies from 0-1000 eV are used for elemental analysis. Because of the low energy of the electrons, the escape probability decreases rapidly as a function of depth. A mean escape depth of 3-8 Å has been estimated for Auger electrons with energies between 0 to 360 eV [51, 52]. The distribution of elements as a function of depth can be readily determined by in situ argon ion etching during Auger analysis. The sensitivity has been found to be sufficient for detecting surface concentrations of less than one atomic percent [50, 51, 53]. Although Auger spectroscopy has been used primarily for elemental analysis, it can be utilized for chemical identifications when the Auger transitions involve valence levels. For example, carbon in the form of graphite, metal carbide, or adsorbed CO can be differentiated by the line shapes of the carbon Auger electron energy distributions [54].

Auger analysis has been used in our laboratory to study the effect of heat treatment on the composition of free surfaces of some high-strength steels. Results on 18Ni(250) maraging steel and AISI 4340 steel are presented as examples. The nominal chemical compositions of these two steels are given in Table 1.

Representative spectra for the 18Ni(250) maraging steels that result from solution annealing and aging treatments are shown in Figure 16. Spectrum A was obtained after cleaning the surface by argon ion etching. Except for the small carbon and oxygen peaks, the composition for the "clean" surface is typical for that expected from the bulk. The

small amounts of carbon and oxygen found after ion cleaning is attributed to adsorption of CO which is one of the principal residual gases in ion-pumped ultrahigh vacuum systems. All of the major elements of this alloy are resolved with the exception of cobalt, because the Auger spectrum for cobalt overlaps the spectra of iron and nickel. The presence of cobalt is indicated, however, by the increased heights of the peaks at 715 eV (Fe) and 775 eV (Ni). Solution annealing at 850°C for one-half hour produced considerable changes in surface composition as indicated by spectrum B. The solution annealing treatment induced segregation of sulfur, carbon and titanium at the surface. The presence of small amounts of nitrogen could not be ascertained since the titanium and nitrogen peaks overlap. The shape of the carbon Auger peak suggests that the carbon is in the form of a carbide. This carbide is most probably TiC because of the higher heat of formation of TiC relative to the carbides of iron and nickel. Precipitation of titanium carbide has been observed at the prior austenite grain boundaries of 18Ni(250) maraging steel [55]. Aging at 500°C for three hours promoted further segregation of titanium and carbon. This aging treatment also induced segregation of molybdenum, which did not occur during annealing. The spectrum of the annealed and aged specimen is shown as spectrum C in Figure 16. These observations indicate that both alloying and residual elements can readily segregate at the boundary surfaces.

Changes in the surface composition of a low alloy (AISI 4340) steel were also determined as a function of thermal treatment to investigate the tendency for the segregation of elements and the precipitation of second phases at the surface. The surface composition as indicated by spectrum A is representative of bulk composition, Figure 17. The specimen was austenitized at 850°C for 15 minutes, cooled to room temperature, and then tempered at 200°C for 1 hr. Auger spectrum for the quenched and tempered material

is shown as spectrum B. The shape of the carbon peak indicates the presence of iron carbide on the surface. Phosphorus, sulfur and nitrogen also segregated at the surface following this treatment. The extent of sulfur segregation for the AISI 4340 steel was considerably less than that found for the 18Ni(250) maraging steel. This difference in the extent of sulfur segregation may be attributed to the higher concentration of maganese in the AISI 4340 steel.

These examples illustrate the changes in surface composition that can result from thermal treatments. The free surface compositional changes shown in Figures 16 and 17, however, do not necessarily represent changes that are produced at internal boundaries of these steels. The observed segregation of elements to the surfaces of 18Ni(250) maraging and AISI 4340 steels do, however, indicate the tendency for certain elements to segregate. The surface compositions of the internal boundaries are also expected to change during thermal treatments. For those cases, in which thermal processing alters the susceptibility to environmentally enhanced fatigue crack growth, without significant alteration of the metallurgical structure of the steel, surface composition may be the determining factor. Thus, it appears necessary to make correlations between susceptibility and surface composition to arrive at the fundamental mechanisms for corrosion fatigue. It must be emphasized that analysis should be conducted on surfaces that are produced during crack growth. Studies are currently in progress in this laboratory to analyze the fracture surfaces of high strength steels that are produced by crack growth in hydrogen and in moisture.

Gas/Metal Surface Reactions

To provide the basis for the surface studies some general aspects of the kinetics of chemisorption and oxidation are summarized in this section. The kinetics of a simple

dissociative chemisorption process on a homogeneous metal surface described by Ehrlich [56] and Smith [57] is discussed first. The factors that must be taken into account for studying chemisorption kinetics of real systems is then discussed. Available information on the reactions of water with clean metal surfaces is also reviewed. In a later section initial results from a current program in our laboratory for measurements of chemisorption rates of oxygen and water vapor and rates of initial oxide formation in these environments are summarized.

The chemisorption process for a diatomic gas, G_2, on a metal surface is represented below:

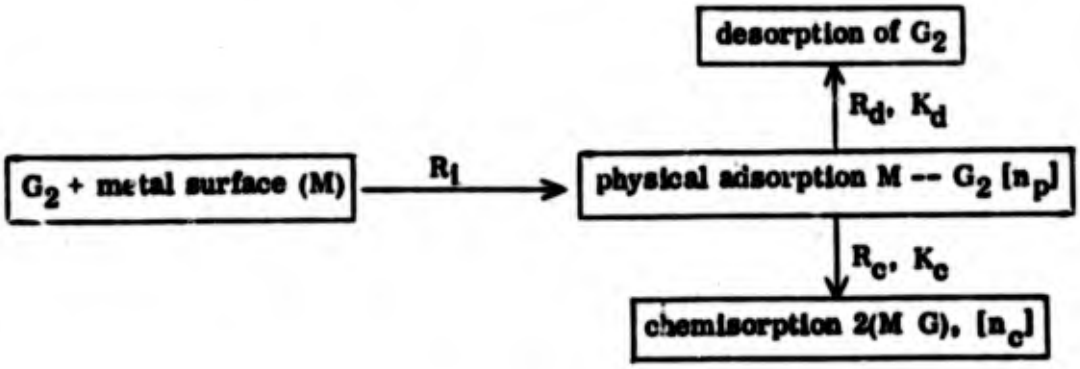

R designates rates, k denotes rate constants and [n] is the concentration of adsorbed species. The impingement rate is found from the kinetic theory of gases and is expressed as

$$R_i = p/(2\pi m/\beta)^{\frac{1}{2}} \qquad (1)$$

where p is pressure, m is the molecular mass and $\beta = 1/kT$. The desorption rate of the physically adsorbed gas, R_d, and the rate of chemisorption, R_c, are determined by the following expressions:

$$R_d = k_d [n_p] \qquad (2)$$

$$R_c = k_c \frac{[n_p]\,[n_o - n_c]^2}{[n_c]^2} \qquad (3)$$

The term $[n_o - n_c]$ is the concentration of available chemisorption sites during the adsorption process, where $[n_o]$ is the total initial concentration of available lattice sites. The coverage, Θ, is defined as the fraction of the available sites that are occupied by chemisorbed species, $\Theta = [n_c]/[n_o]$. The reaction rate is written in terms of coverage as

$$R_c = k_c [n_p] (1 - \Theta)^2 \tag{4}$$

The rate of chemisorption can be expressed in more convenient terms by eliminating $[n_p]$ from the above expression. The rate of change in the concentration of physically adsorbed molecules, $[n_p]$, depends upon the impingement rate and the rates of removal by desorption and chemisorption. Assuming a steady state for the concentration $[n_p]$, i.e., $d[n_p]/dt \cong 0$, then $[n_p]$ can be obtained from the following relationship:

$$\frac{d[n_p]}{dt} = R_i - R_d - R_c = \frac{p}{(2\pi m/\beta)^{\frac{1}{2}}} - k_d [n_p] - k_c [n_p] (1 - \Theta)^2 = 0 \tag{5}$$

When the resulting expression for $[n_p]$ is introduced into equation (4), R_c becomes

$$R_c = \left[\frac{p}{(2\pi m/\beta)^{\frac{1}{2}}}\right]\left[\frac{1}{1 + \frac{1}{(1 - \Theta)^2}\frac{k_d}{k_c}}\right] \tag{6}$$

In transferring the physically adsorbed molecules into the chemisorbed state, the number of successful events will depend upon an activation energy, E_c, a probability factor, γ_c, and the vibration frequency perpendicular to the surface, ν_c. The reaction constant for chemisorption can then be expressed as $k_c = \gamma_c \nu_c \exp(-E_c\beta)$. Similarly, the desorption rate constant can be written as $k_d = \gamma_d \nu_d \exp(-E_d\beta)$. Substituting these rate constants into equation (6), the chemisorption rate is given by:

$$R_c = \left[\frac{p}{(2\pi m/\beta)^{\frac{1}{2}}}\right]\left[\frac{1}{1 + \frac{1}{(1-\Theta)^2}\,\frac{\sigma_d \nu_d}{\sigma_c \nu_c}\,\exp\left[(E_c - E_d)\beta\right]}\right] \qquad (7)$$

This relationship shows the functional dependence of chemisorption rate on temperature, pressure and coverage.

The second bracketed term in equation (7) is the sticking coefficient, S, which denotes the fraction of the impinging molecules that is chemisorbed. The variation in the sticking coefficient with temperature at constant coverage can be examined in terms of the experimentally accessible quantity $S/(1 - S)$

$$\left[\frac{\partial \ln S/(1-S)}{\partial \beta}\right]_\Theta = E_d - E_c \qquad (8)$$

A rise in temperature can, therefore, result in either an increase or a decrease in the chemisorption rate depending on the relative activation energy of desorption, E_d, and the activation energy of chemisorption, E_c. The activation energy for transformation from the physically adsorbed state to the chemically bound state, E_c, can be derived from the rate variation with temperature only if E_d is known, or if $E_c >> E_d$.

The fundamental assumptions for this formulation do not take into account the effects of induced and existing surface heterogeneity. For real surfaces, the rate of chemisorption depends upon the distribution of sites, and upon the kinetics of chemisorption and physical adsorption at each of these sites. The variation of the sticking coefficient for a gas on a heterogeneous surface, therefore, may not be a simple function of temperature. Although it is unlikely that equations (7) and (8) provide a quantitative description of chemisorption kinetics for actual experimental conditions, qualitative predictions can be made for the dependence of chemisorption rates on T, p, and Θ. The

rates of surface and bulk diffusion of adsorbed species have not been included in this consideration of chemisorption kinetics. These rates must be incorporated in a more complete formulation.

Studies of the reaction of water with clean metal surfaces have been made on Ni [58], Cu [59, 60], Fe [58, 61], Al [62], Pt [63], Mo [64] and W [65-68] (of these , work on the W/H_2O system has been the most extensive). Dissociative chemisorption of water has been observed on all of these metals and results in the formation of chemisorbed hydrogen and/or the evolution of hydrogen. The results of these studies will be used to illustrate the general behavior of water at clean metal surfaces. It is recognized, however, that there may be differences in detail between specific metal/water systems.

A number of investigations, particularly on the W/H_2O system, have indicated that water adsorbs by the following processes [63, 65, 66]:

$$\text{Step I} \qquad H_2O + 2M \longrightarrow MH + MOH$$

$$\text{Step II} \qquad H_2O + MH \longrightarrow MOH + H_2\uparrow$$

The occurrence of Step I has been established by resistivity and work function measurements [63, 65]. The reaction indicated by Step II has been deduced from the observation that hydrogen evolution does not take place until a "threshold" coverage is reached [61, 65]. Waclawski and Hughey [65] found that the rate of hydrogen evolution in the W/H_2O system was limited by the water vapor pressure in accordance with Step II. These authors suggested that the high mobility of hydrogen allows easy migration to secondary sites at low coverages. As these secondary sites become filled with OH groups, the impinging H_2O molecules have a higher probability for desorbing hydrogen by replacement or by reaction. Thermal desorption studies by Ustinov and Ivanov [67] have provided further details for the mechanism of chemisorption of water on metal surfaces. Water was

found to chemisorb on tungsten in three states at room temperature. These adsorption states are, in increasing order of their activation energies for desorption, α, β_1, and β_2. The α state represents chemisorbed H_2O molecules, and the β states involve the adsorption of dissociated water. Initially, adsorption in states α and β_2 occurs simultaneously on a clean surface. The water molecules in the α state, however, are very mobile and pass rapidly into the β_2 state. The accumulation of molecular H_2O, the α state, on the surface occurs only after most of the sites in the β_2 state have been filled. As H_2O concentration in the α state approaches the equilibrium value, the β_1 state (having the highest activation energy for adsorption) then begins to fill. These results indicate that the reaction represented by Step I may be preceded by the chemisorption of molecular water. The dissociative adsorption of water indicated by Step I likely corresponds to the filling of the β_2 state. If one assumes that the chemisorption into the β_1 state is associated with the reaction in Step II, then the thermal desorption studies would indicate that this step requires an activation energy.

Inai and Kemball [66] have also suggested that adsorption of water on clean tungsten follows Steps I and II. Furthermore, they investigated the influence of oxygen on the H_2O/W reactions. Oxygen was observed to displace adsorbed hydrogen from both water and hydrogen treated surfaces. At 0°C neither water nor hydrogen, on the other hand, was found to react appreciably with tungsten surfaces that have pre-adsorbed oxygen. These results imply that oxygen may inhibit the reaction of water vapor with surfaces created at the fatigue crack tip.

The initial dissociative chemisorption of water vapor on metal surfaces is the only mechanism considered thus far for causing "embrittlement." The later stages of water metal reactions must also be considered as a possible mechanism for influencing crack

growth. The chemisorption of reactive gases on metals, in many cases, is followed by a slow activated incorporation of the chemisorbed species into the metal [69]. This second stage of chemisorption for oxygen and for water may be associated with initial oxide formation. Evidence for the oxidation of clean metal surfaces by water vapor has been reported by Inai and Kemball [66] for tungsten and by Chang and Wade [61] for iron. Inai and Kemball [66] observed that when water vapor was chemisorbed onto clean tungsten at 0°C, there was a one-to-one correspondence between the amount of hydrogen evolved and the number of surface sites. At 100-200°C, however, the amount of hydrogen produced in the reaction was higher than the number of surface tungsten atoms. The authors suggested that at these high temperatures the surface had oxidized to a mixture of WO_2 and WO_2H. Similar results were found for iron by Chang and Wade [61]. Formation of 4 to 10 "equivalent" layers of FeO was observed for the reaction of water vapor with evaporated iron film at 24°C.

The enhancement of crack growth by water/water vapor results from chemisorption and/or initial oxidation of the newly created crack surface. The mechanisms for inducing crack growth may be related to hydrogen produced by these reactions or to oxidation per se. To correlate the details of surface reactions with the effects of fatigue testing variables, concurrent surface chemistry and corrosion fatigue studies on identical materials would be most rewarding. For example, if hydrogen is the principal cause for "embrittlement," then the adsorption mechanism described by reactions I and II may be important. The reaction indicated by Step I produces chemisorbed hydrogen which can readily induce "embrittlement." The reaction of Step II, however, causes the desorption of hydrogen, thus making it less accessible to the crack tip. Based on these considerations, water would be expected to have a maximum effect on crack-growth under testing conditions

that allowed sufficient time for reaction I to take place, but inhibited reaction II. These conditions may exist under certain test frequencies and applied waveforms [4, 16, 17, 25, 26]. Studies should, of course, include considerations of mechanisms other than those related to hydrogen. The influence of oxygen on the reactions of water vapor with metal surfaces must be examined to resolve the discrepancies between observations on the inhibiting effect of oxygen on crack-growth in high-strength steels in humid environments [18, 35]. The influence of surface composition on surface reactions must also be considered in relating surface chemistry to fatigue crack growth in specific steel-environment systems.

V. CHEMISORPTION STUDIES ON IRON AND STEEL SURFACES

A research program is in progress in this laboratory to carry out many of the studies suggested in the previous sections. Initial studies have been directed at the reactions of oxygen with iron and steel. The results of these studies are described in this section. The reactions were followed by monitoring the oxygen Auger peak intensity as a function of time and oxygen pressure. The oxygen peak intensity was calibrated in terms of adsorbed amount of by assuming that the initial sticking probability, S, is unity as reported by Horgan and King [70]. The reaction rates of oxygen with clean surfaces of iron single crystals serve as a reference for investigations of other surfaces with different compositions and morphology. The results of oxygen chemisorption studies on AISI 4340 steel and clean Fe(001) are discussed.

The initial rate of chemisorption of oxygen on clean Fe(001) surface is shown in Figure 18. The sticking coefficient is constant up to an oxygen coverage of approximately 0.9×10^{15} atoms/cm^2, and decreases gradually for higher coverages. If one assumes that the number of chemisorption sites is equal to the number of surface iron atoms,* then the inflection in the coverage vs. exposure curve occurs near the completion of a monolayer. For exposures between 2 to 8×10^{-6} torr-sec the specimen continues to take-up oxygen, but at rates slower than the initial rate. The adsorption rate increases again for exposures between 8 to 24×10^{-6} torr-sec and then continues to decrease exponentially for exposures above 24×10^{-6} torr-sec., Figure 19. These results are in qualitative agreement with the observed changes in sticking coefficient with coverage for oxygen on clean evaporated iron films [70].

---

* The surface density of iron atoms in Fe(001) is 1.22×10^{15} atoms/cm^2

The second stage of adsorption, at exposures above 2×10^{-6} torr-sec., is interpreted to be associated with initiation of oxidation. To provide further evidence for this interpretation, the intensity of the 598 eV Fe peak was monitored as a function of oxygen adsorption. These data were normalized by dividing the Fe peak intensity at specific coverages by the Fe peak intensity for a clean surface (Fe/Fe_o). As the oxide grows in thickness the ratio (Fe/Fe_o) should approach the limiting value of (D_1/D_2) (δ_2/δ_1), where D_1 and D_2 are the atomic densities of iron in the oxide and metal phases respectively, and δ_1 and δ_2 are the corresponding linear attenuation coefficients for 598 eV electrons [72]. The decrease of (Fe/Fe_o) ratio with the onset of the second stage of oxygen adsorption, Figure 19, tends to support the interpretation that this stage of adsorption represents oxide formation. This observation may be compared with the results of Sewell et al. [71]. These authors studied the early stages of oxidation for a Fe(001) surface by electron diffraction and by X-ray emission. They observed no new diffraction features up to oxygen exposures of 10×10^{-6} torr sec. A fcc NaCl type surface structure developed at oxygen exposures of 12 to 15×10^{-6} torr-sec corresponding to coverages of between 2.4 and 3.7×10^{15} atoms/cm.^{2} Exposures and coverages for the formation of the initial oxide are comparable to those at which (Fe/Fe_o) decreased and a distinct change in the adsorption rate was observed. It is concluded, therefore, that the results shown in Figures 18 and 19 depict the chemisorption of a monolayer of oxygen for exposures between 0 to 2×10^{-6} torr-sec and that the rate of chemisorption for higher exposures corresponds to the rate of initial oxidation.

SUMMARY

Available experimental data indicate that fatigue crack growth behavior in high-strength steels may be broadly separated into two regions, delineated in relation to their stress corrosion cracking characteristics; one region above the so-called apparent threshold stress intensity for stress corrosion cracking, K_{Iscc}, and the other, below K_{Iscc}. The dependence on loading variables, such as frequency, stress ratio and waveform in the region above K_{Iscc} can be very strong and appears to be related to the environment sensitivity of the steels. The effects of these loading variables, above K_{Iscc}, can be accounted for reasonably well by a superposition model that utilizes crack growth data under sustained loading, that is, data for stress corrosion cracking. The close correlation between the rates of crack growth under sustained and cyclic loadings demonstrates the intimate relationship between the mechanism(s) for stress corrosion cracking and corrosion fatigue. Separate studies of the mechanism(s) for corrosion fatigue and stress corrosion cracking appear to be unnecessary. Below K_{Iscc}, it has been shown that the environmental effects are still present. The effects are also functions of frequency, stress ratio and waveform. The behavior is, however, much more complex. For example, the environmental effect is minimal at both low and high frequencies, and exhibits a maximum at some intermediate frequency. Certain waveforms produce enhancement in crack growth while others show little effect. No direct correlation with stress corrosion data is possible, since these effects occur at K levels below the apparent stress corrosion cracking threshold, K_{Iscc}. A more detailed understanding of the chemical and mechanical processes for corrosion fatigue is required.

Recent work on the kinetics of crack growth has shown that a number of nonsteady state phenomena, such as transient growth, incubation and crack acceleration, can occur under sustained loading. Nonsteady-state crack growth has also been observed in fatigue.

These nonsteady state phenomena are unquestionably related to the kinetics of surface reactions and to hydrogen diffusion, and need to be understood.

Further progress in understanding the phenomenology and mechanism(s) for corrosion fatigue requires more quantitative information on both the chemical and mechanical processes involved. Review of mechanisms for water/metal interactions indicates that further quantitative studies of surface reaction will provide definitive correlation between surface chemistry and the effects of loading variables on crack growth. The Auger technique appears to be an effective method for surface characterization and for following the reaction of gases with iron and steel. Chemisorption experiments for oxygen and water vapor on iron and on AISI 4340 steel, and studies of fatigue crack growth kinetics in AISI 4340 steel are in progress.

ACKNOWLEDGMENT

Support of this work by the Office of Naval Research through Contract Nonr N00014-67-A-0370-0008, NR 036-097, is greatfully acknowledged.

TABLE I

COMPOSITIONS OF HIGH STRENGTH STEELS (wt. %)

	C	Mn	P	S	Si	Ni	Cr	Mo	Co	Ti
18 Ni 250 Maraging	0.002	--	0.001	.002	0.002	18.0	--	5.0	7.5	0.4
AISI 4340	0.42	0.70	0.0009	.0012	0.28	1.83	0.79	0.24	0.011	<0.005

REFERENCES

1. P. B. Haigh, J. Inst. Metals 18, 55 (1917).

2. A. J. McEvily, Jr. and R. P. Wei, Proceedings - International Conference on Corrosion Fatigue, University of Connecticut, 1971, NACE, 381 (1972).

3. J. P. Gallagher and R. P. Wei, ibid, 409.

4. J. M. Barsom, ibid, 424.

5. R. P. Wei and M. O. Speidel, ibid, 379.

6. A. J. McEvily, Jr. and W. Illg, NACA TN 4394 (1958).

7. J. A. Feeney, J. C. McMillan and R. P. Wei, Met. Trans. 1, 1741 (1970).

8. P. C. Paris, R. J. Bucci, E. T. Wessel, W. G. Clark, Jr. and T. R. Mager, ASTM STP 513 (1972).

9. R. J. Bucci, W. G. Clark, Jr. and P. C. Paris, ASTM STP 513 (1972).

10. B. F. Brown and C. D. Beachem, Corrosion Science 5, 745 (1965).

11. R. P. Wei, S. R. Novak and D. P. Williams, Mat'l. Res. & Std., ASTM 12, 25 (1972).

12. R. P. Wei, J. Eng'g. Fract. Mech. 1, 633 (1970).

13. R. P. Wei and J. D. Landes, Mat'l. Res. & Std., ASTM 9, 25 (July 1969).

14. F. J. Bradshaw and C. Wheeler, RAE TR-68041 (February 1968).

15. R. Bucci, Ph. D. Dissertation, Lehigh University (1970).

16. J. M. Barsom, Ph. D. Dissertation, University of Pittsburgh (1969).

17. G. A. Miller, S. J. Hudak, Jr. and R. P. Wei, "The Influence of Loading Variables on Environment-Enhanced Fatigue Crack Growth in High Strength Steels," to be published by ASTM (copies available from authors on request).

18. R. P. Wei, P. M. Talda and Che-Yu Li, ASTM STP 415, 460 (1967).

19. W. A. Spitzig, P. M. Talda and R. P. Wei, J. Eng'g. Fract. Mech. 1, 155 (1968).

20. G. A. Miller, Trans. ASM 61 (1968).

21. J. D. Landes, Ph. D. Dissertation, Lehigh University (1970).

22. W. A Spitzig and R. P. Wei, J. Eng'g. Fract. Mech. 1, 719 (1970).

23. D. A. Meyn, Rept. NRL Progress, 14 (February 1968).

24. J. H. FitzGerald and R. P. Wei, "A Test Procedure and Analysis of the Influence of Stress Ratio on Fatigue Crack Growth," submitted for publication by ASTM (copies available from authors).

25. F. J. Bradshaw, N. J. F. Nunn and C. Wheeler, RAE Tech. Memo, MAT 93 (July 1970).

26. S. J. Hudak, Jr. and R. P. Wei, Proceedings - International Conference on Corrosion Fatigue, University of Connecticut, 1971, NACE, 433 (1972).

27. E. P. Dahlberg, Trans. ASM 58, 46 (1965).

28. E. J. Imhof, Jr. and J. M. Barsom, "Fatigue and Corrosion-Fatigue Crack Growth of 4340 Steel at Various Yield Strengths," presented at the Sixth National Symposium on Fracture Mechanics, Philadelphia, Pa., August 28-30, 1972.

29. A. J. Baker, F. J. Lauta and R. P. Wei, ASTM STP 370, 3 (1965).

30. R. P. Wei, Int'l. J. Fract. Mech. 4, 159 (1968).

31. F. Jeglic, P. Neissen and D. J. Burns, "Temperature Dependence of Fatigue Crack Propagation in an Al-2.6% Mg Alloy," presented at the Symposium on Fatigue at Elevated Temperatures, University of Connecticut, June 18-22, 1972.

32. J. T. Ryder and J. P. Gallagher, Trans. ASME, Ser. D., 92, 121 (1970).

33. A. J. McEvily, Jr. and A. P. Bond, in Environment Sensitive Mechanical Behavior, AIME 35 (1966).

34. H. H. Johnson and A. M. Willner, Appl. Mat'l. Res. 4, 34 (1965).

35. G. G. Hancock and H. H. Johnson, Trans. Met. Soc. AIME, 236, 513 (1966).

36. G. L. Hanna, A. R. Troiano and E. A. Steigerwald, Trans. ASM, 57, 658 (1964).

37. A. W. Van der Sluys, Trans. ASME, Ser. D, 89, 28 (1967).

38. D. P. Williams and H. G. Nelson, Met. Trans., 1, 63 (1970).

39. H. G. Nelson, D. P. Williams and A. S. Tetelman, Met. Trans. 2, 953 (1971).

40. S. J. Hudak, Jr., "The Kinetics of Hydrogen Enhanced Crack Growth in High Strength Steels," M.S. Thesis, Lehigh University (1972).

41. J. W. Cahn and J. E. Hilliard, Acta Met. 7, 219 (1959).

42. D. McLean, Grain Boundaries in Metals, Oxford, 116 (1957).

43. K. T. Aust, R. E. Hanneman, P. Niessen and J. H. Westbrook, Acta Met. 16, 291 (1968).

44. R. E. Hanneman and T. R. Anthony, Acta Met. 17, 1133 (1969).

45. J. M. Capus, "The Mechanism of Temper Brittleness," Temper Embrittlement in Steel, ASTM STP 407, 3 (1968).

46. A. Joshi and D. F. Stein, "Temper Embrittlement of Low Alloy Steels," Temper Embrittlement of Alloy Steels, ASTM STP 499, 59 (1972).

47. A. Joshi and D. F. Stein, Corrosion 28, No. 9, 321 (1972).

48. L. A. Harris, J. Appl. Phys. 39, 1419 (1968).

49. C. C. Chang, Surf. Sci. 25, 53 (1971).

50. G. W. Simmons, J. Coll. Interface Sci. 34, 343 (1970).

51. P. W. Palmberg and T. N. Rhodin, J. Appl. Phys. 39, 2425 (1968).

52. J. M. Chang and D. K. Skinner, Surf. Sci. 19, 283 (1970).

53. M. Perdereau, Surf. Sci. 24, 239 (1971).

54. T. W. Haas, J. T. Grant and G. J. Dooley, J. Appl. Phys. 43, 1853 (1972).

55. C. J. Barton, et al., "Investigation of Thermal Embrittlement in 18Ni(250) Maraging Steel," Technical Report AFML-TR-67-34 (1967).

56. G. Ehrlich, J. Phys. Chem. 59, 473 (1955).

57. T. Smith, J. Chem. Phys. 40, 1805 (1964).

58. R. Suhrmann, J. M. Heras, L. V. Heras and G. Weder, Ber. Bunsenges. Physik. Chem. 68, 511 (1964).

59. R. Suhrmann, J. M. Heras, L. V. Heras and G. Wedler, Ber. Bunsenges. Physik. Chem. 72, 855 (1968).

60. G. Ertl, Surf. Sci. 7, 309 (1967).

61. S. Chang and W. H. Wade, J. Coll. and Interface Sci. 34 (1970).

62. E. E. Huber, Jr. and C. T. Kirk, Jr., Surf. Sci. 5, 447 (1966).

63. C. W. Jowett, P. J. Dobsen and B. J. Hopkins, Surf. Sci. 17, 474 (1969).

64. A. Klopfer, Surf. Sci. 20, 129 (1970).

65. B. J. Waclawski and L. R. Hughey, Surf. Sci. 19, 464 (1970).

66. H. Inai and C. Kemball, Proc. Royal Soc. (London) A302, 399 (1968).

67. Y. K. Ustinov and W. L. Ionov, Sov. Phys. Tech. Phys. 12, 1506 (1968).

68. R. J. Hill, Vacuum 11, 260 (1961).

69. M. A. H. Landon and B. M. W. Trapnell, Proc. Royal Soc. (London) A227, 387 (1955).

70. A. M. Horgan and D. A. King, Surf. Sci. 23, 259 (1970).

71. P. B. Sewell, D. F. Mitchell and M. Cohen, Surf. Sci. 33, 535 (1972).

72. T. A. Carlson and G. E. McGuire, J. Electron Spectroscopy 1, 161 (1972/73).

LIST OF FIGURES

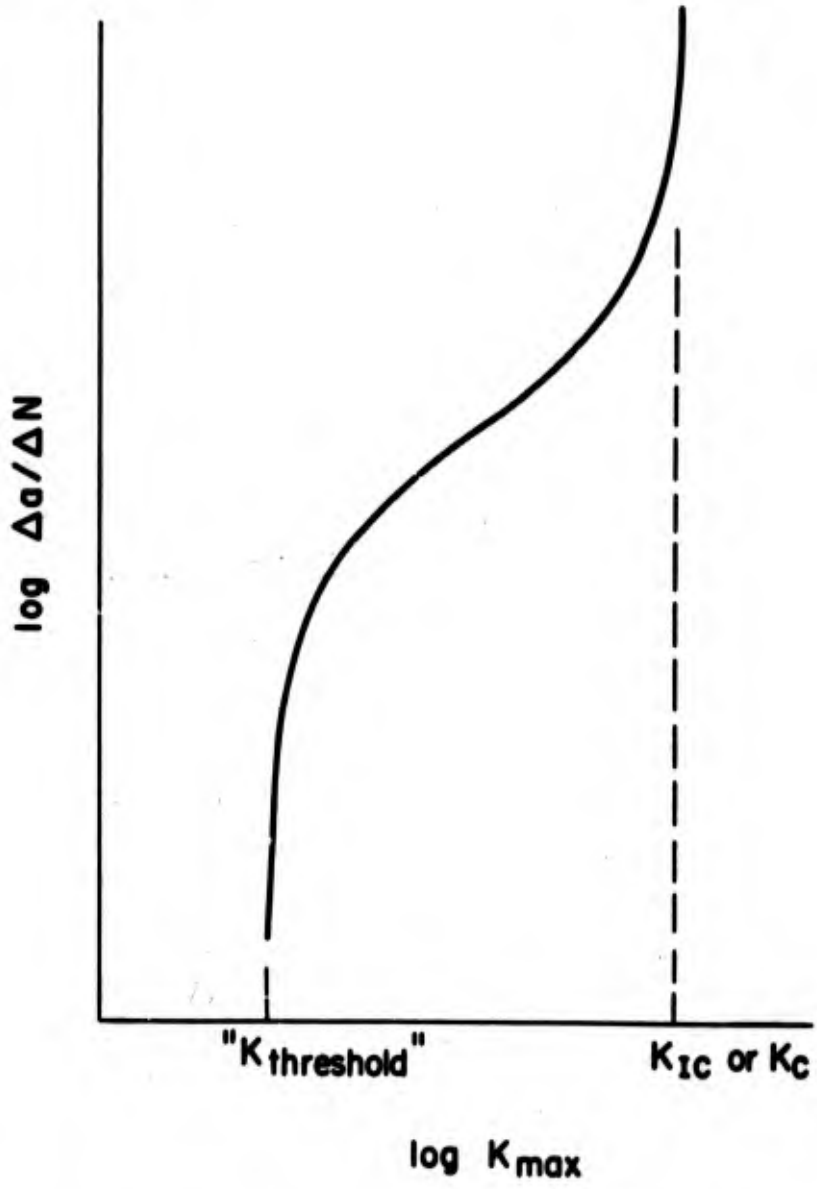

Figure 1: Schematic Representation of Fatigue Crack Growth Kinetics

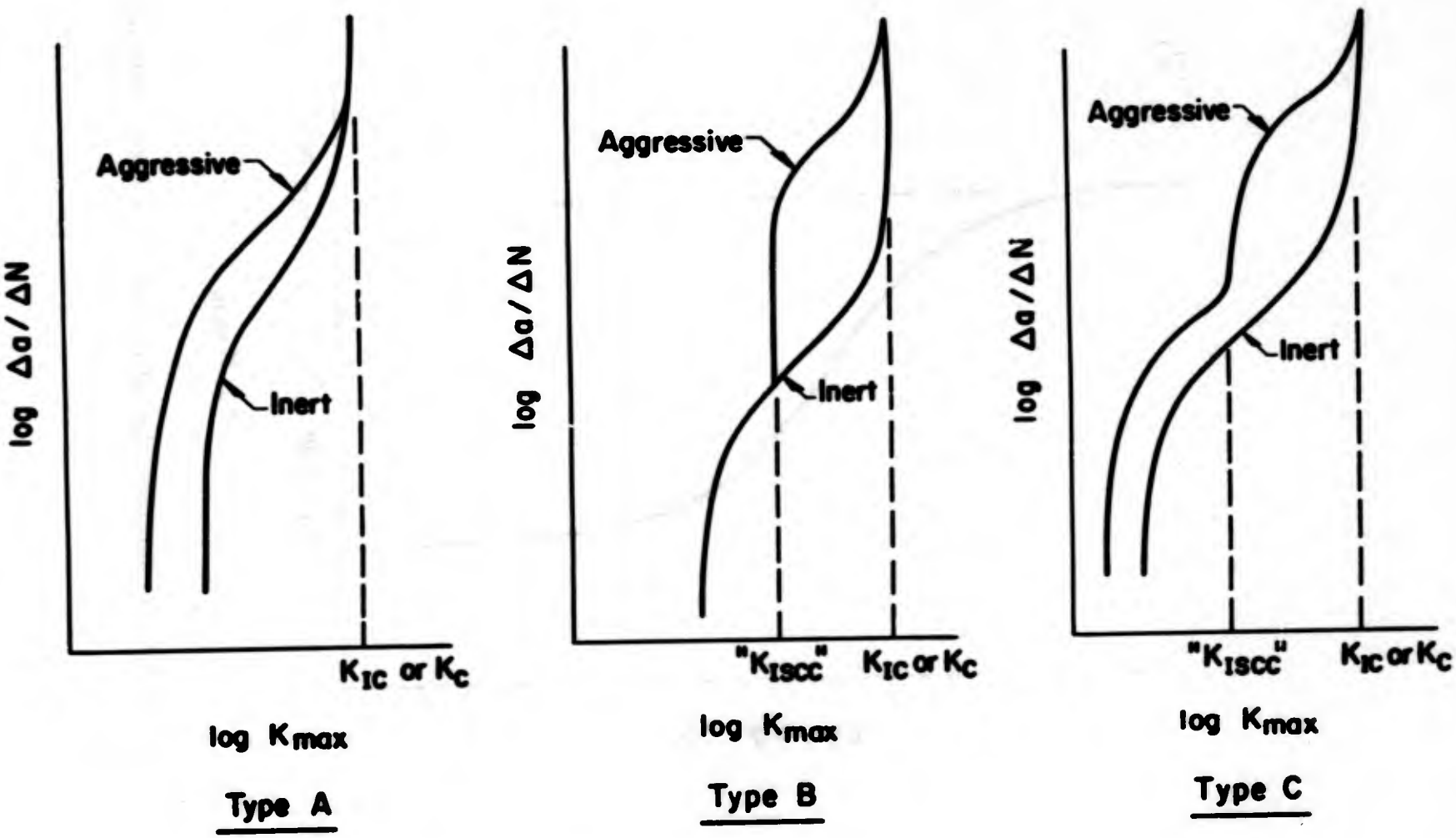

Figure 2: Types of Fatigue Crack Growth Behavior

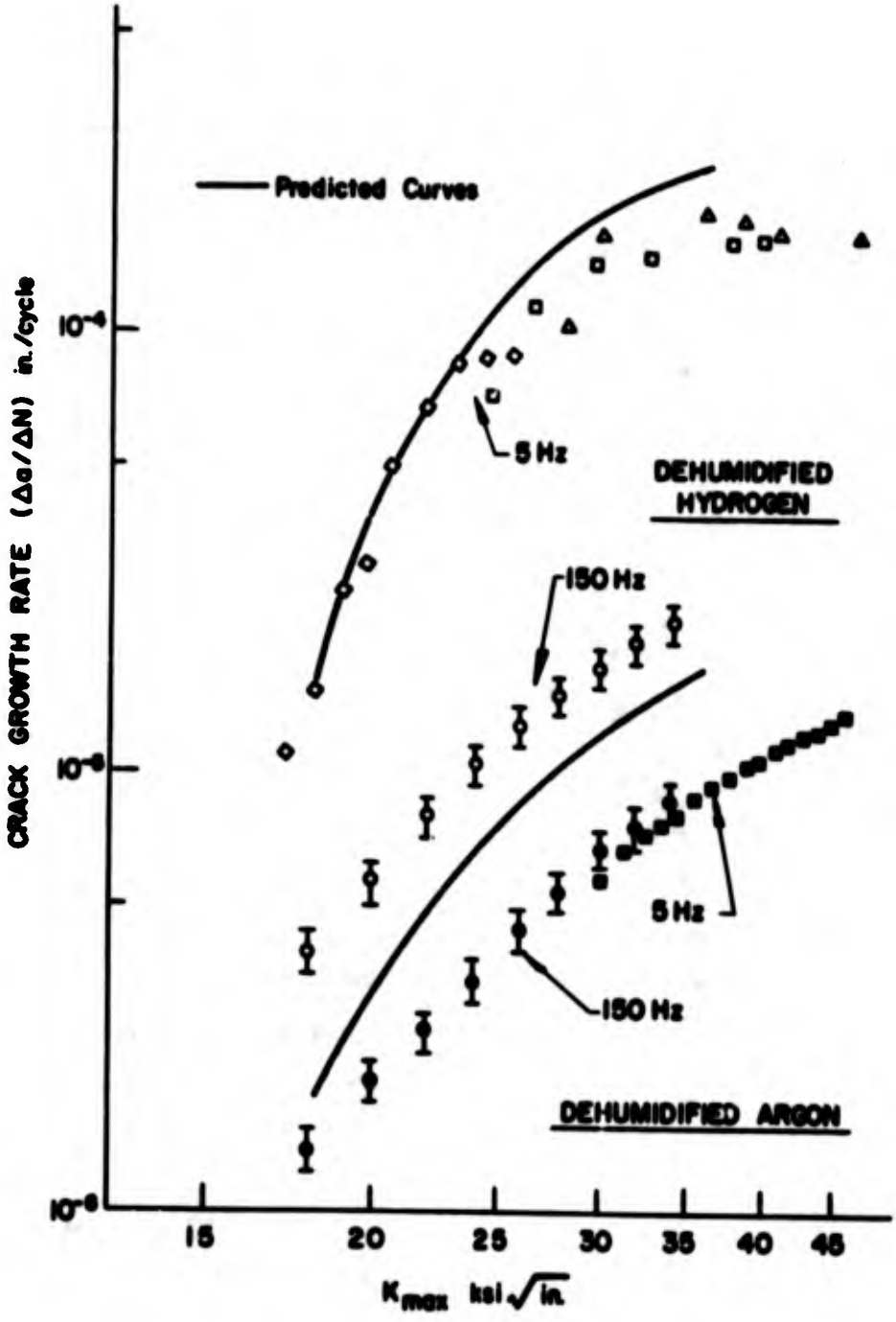

Figure 3: The Effect of Frequency on Fatigue Crack Growth Kinetics (above K_{Iscc}) for 18Ni(250) Maraging Steel, R 0.1 [13].

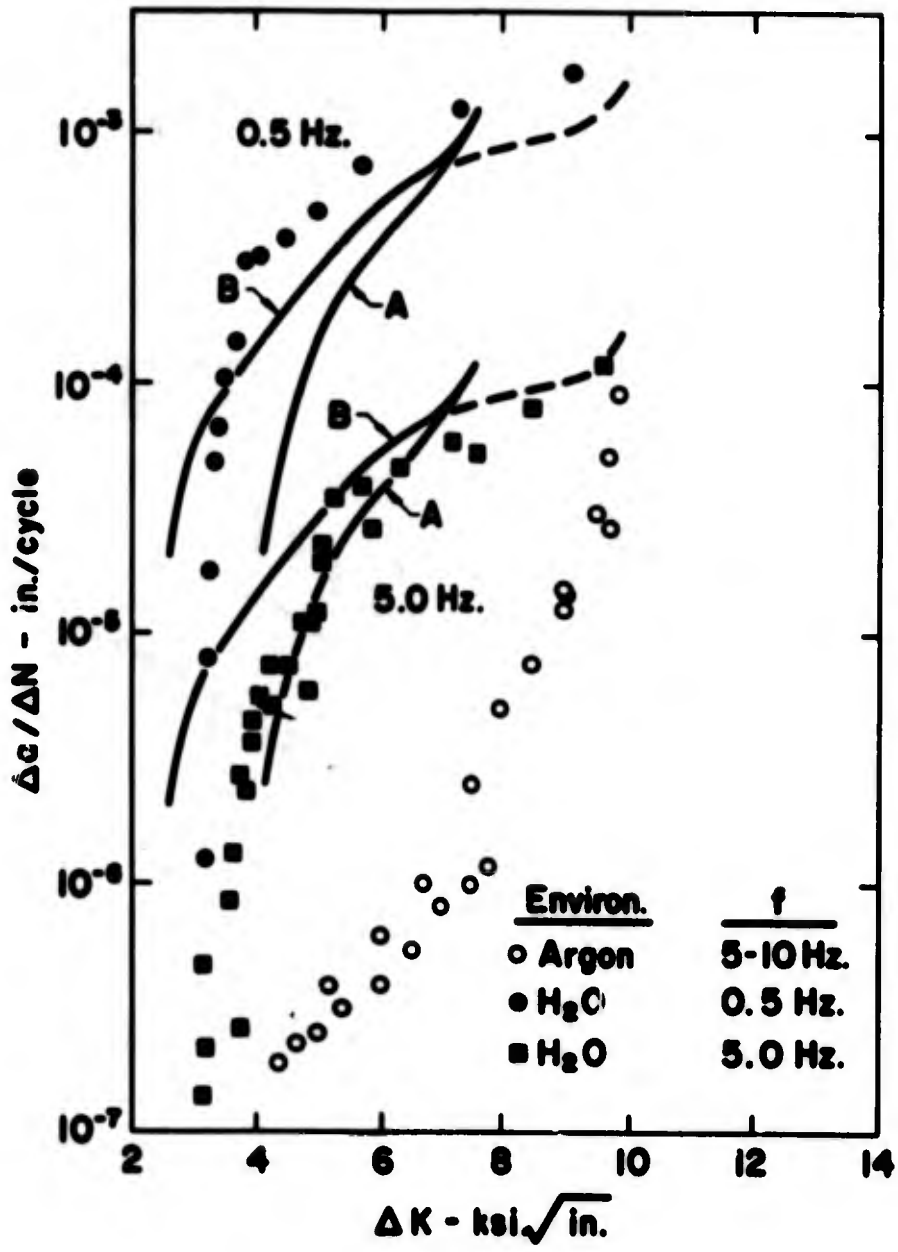

Figure 4: The Effect of Frequency on Fatigue Crack Growth Kinetics (above K_{Iscc}) for AISI 4340 Steel Tempered at 200°F, R = 0.8 ($K_{Iscc} \approx$ 10 to 15 ksi √in.) [17].

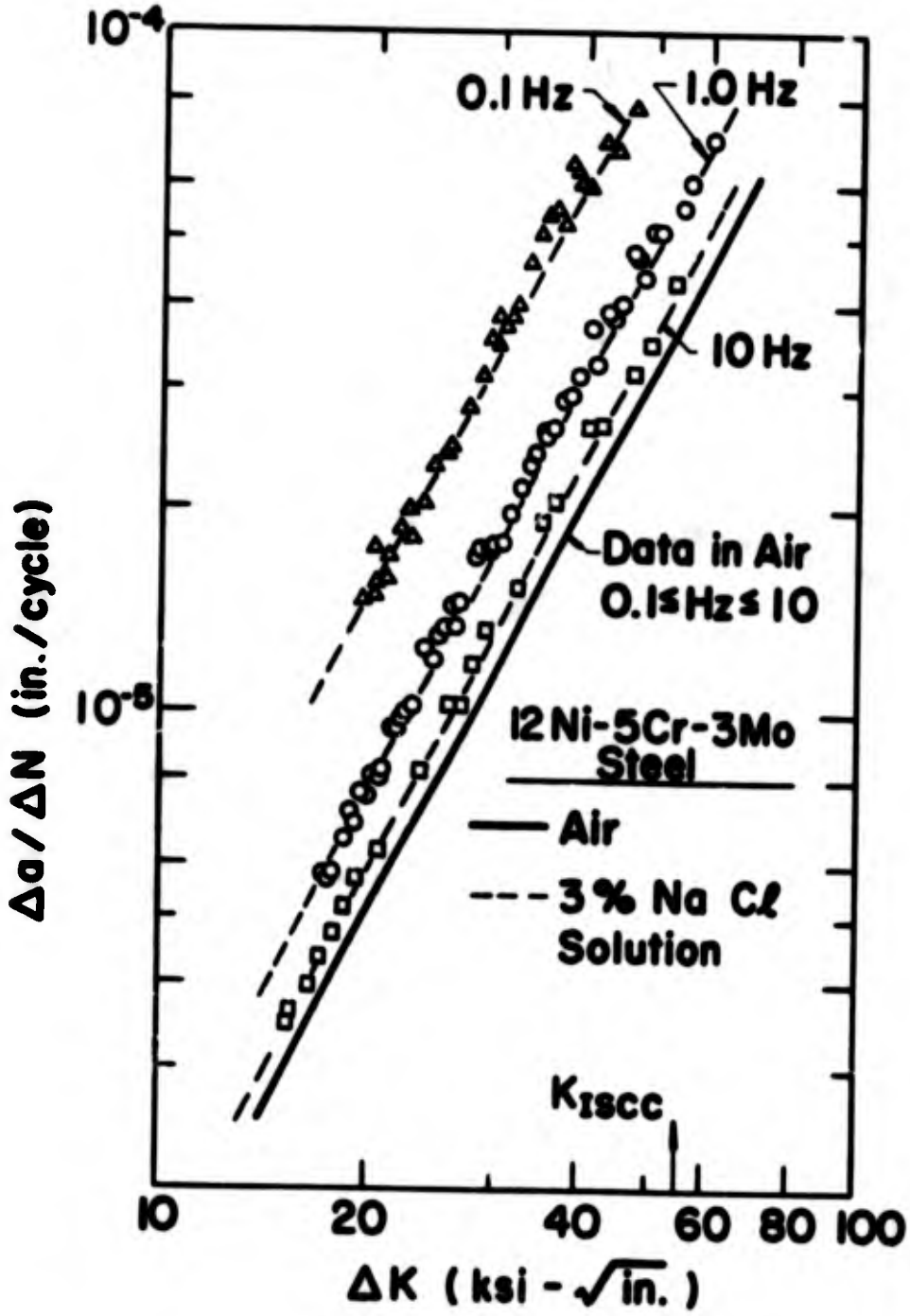

Figure 5: The Effect of Frequency on Fatigue Crack Growth Kinetics (below K_{Iscc}) for 12Ni-5Cr-3Mo Steel [16].

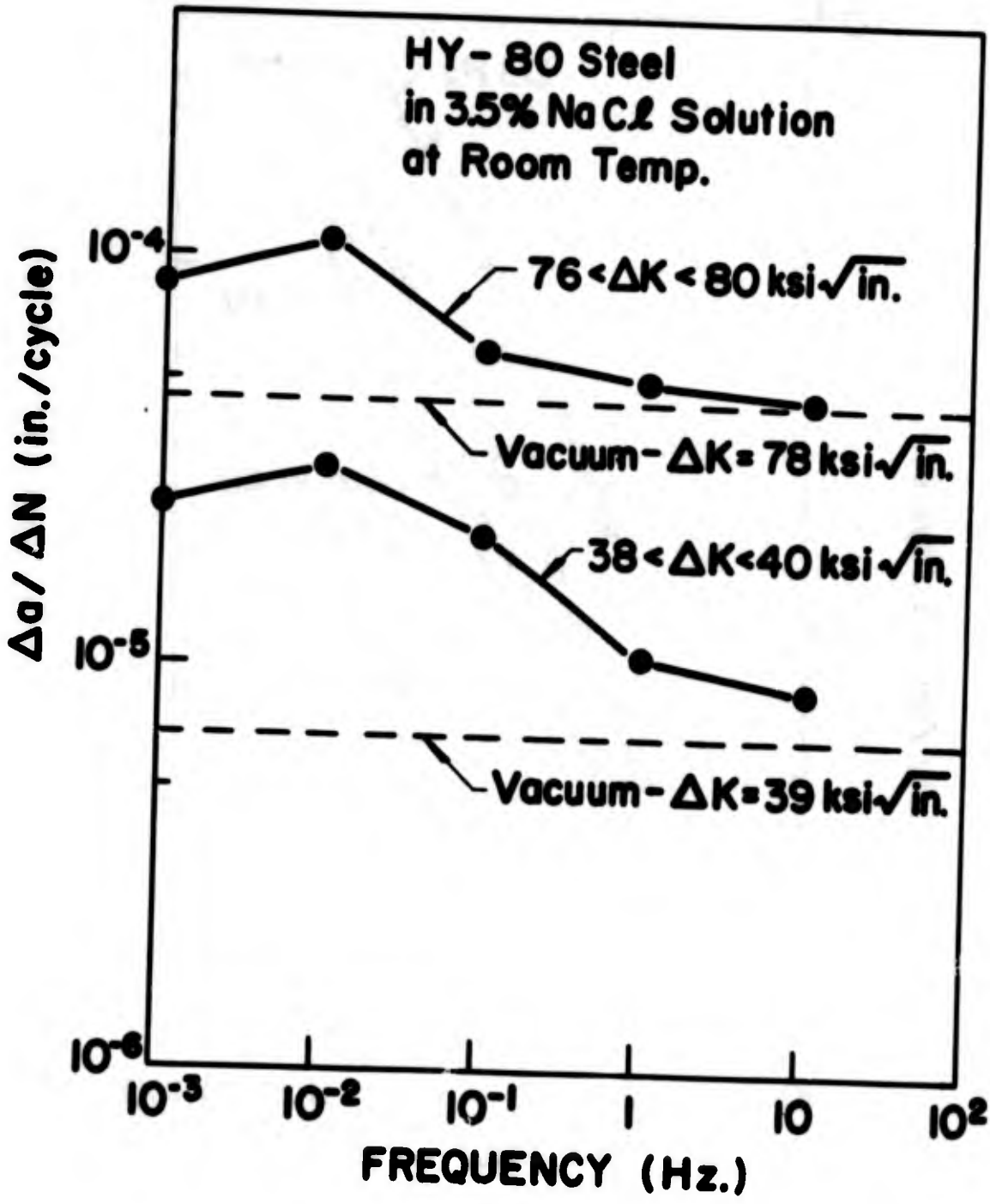

Figure 6: The Effect of Frequency on Fatigue Crack Growth (below K_{Iscc}) for HY-80 Steel [3].

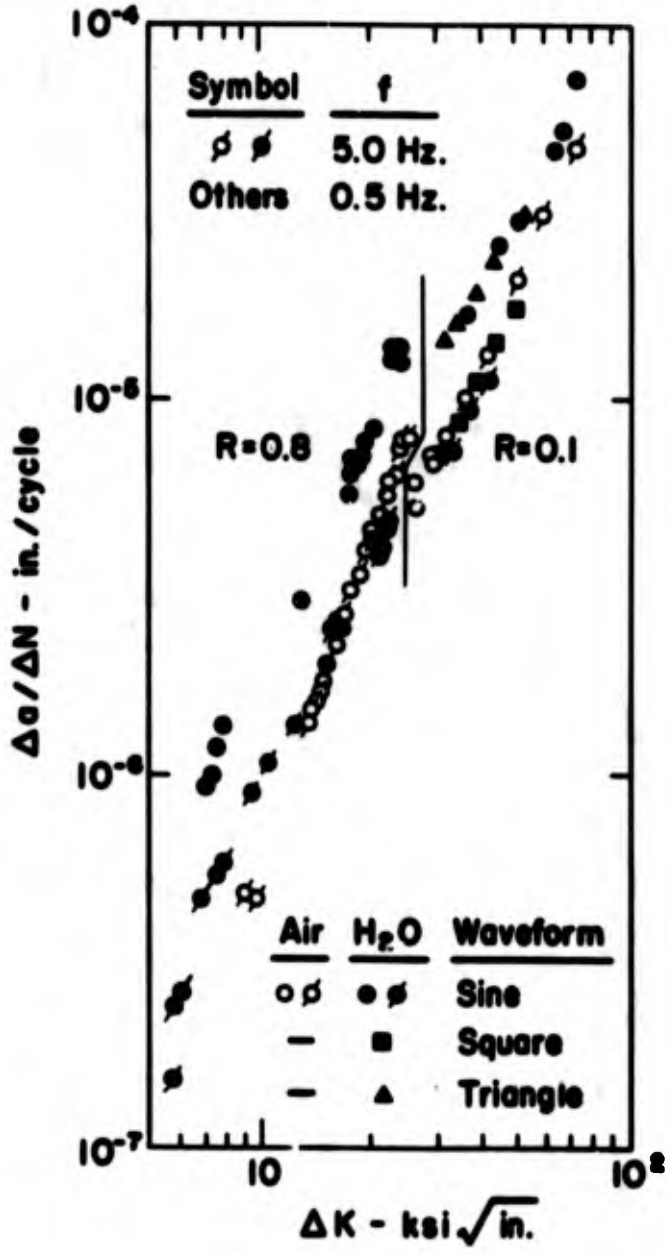

Figure 7: The Effects of Frequency and Waveform on Fatigue Crack Growth Kinetics (below K_{Iscc}) for RQ 360A Steel (ΔK_{Iscc} > 100 ksi √in.) [17].

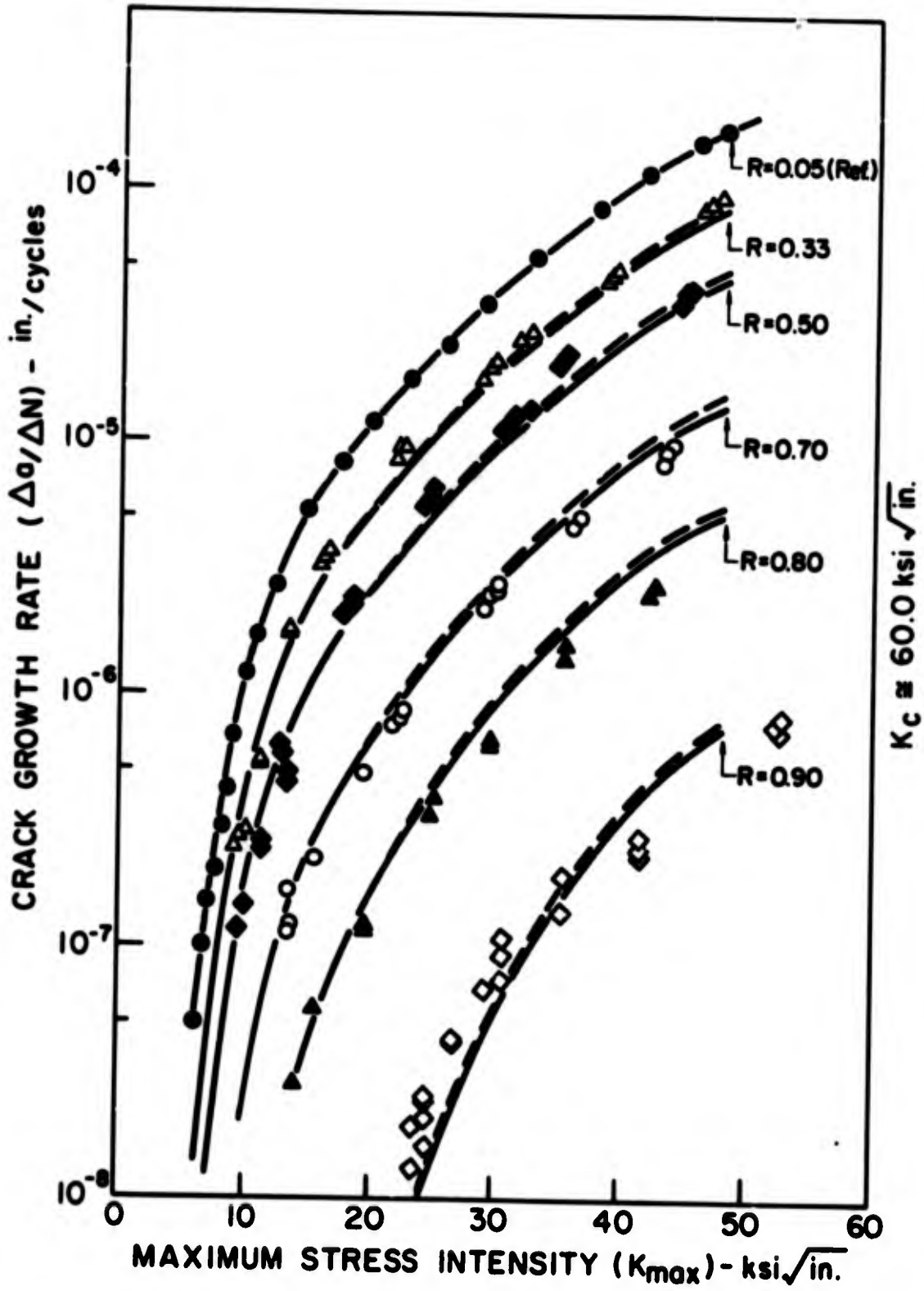

Figure 8(a): Fatigue Crack Growth Kinetics for Ti-6Al-4V Alloy Illustrating the Effect of Stress Ratio in Terms of K_{max} [24].

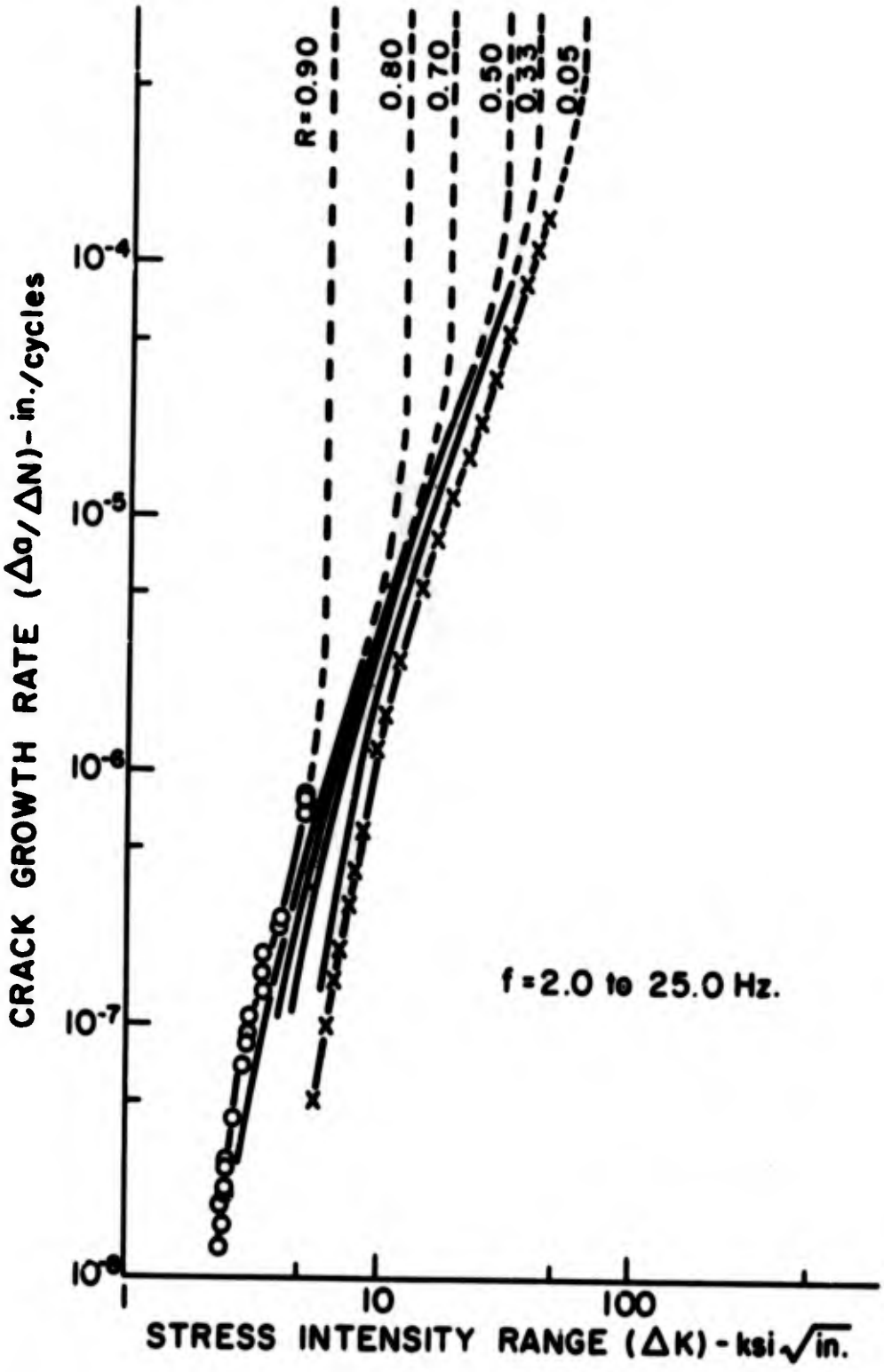

Figure 8(b): Fatigue Crack Growth Kinetics for Ti-6Al-4V Alloy Illustrating the Effect of Stress Ratio in Terms of ΔK [24].

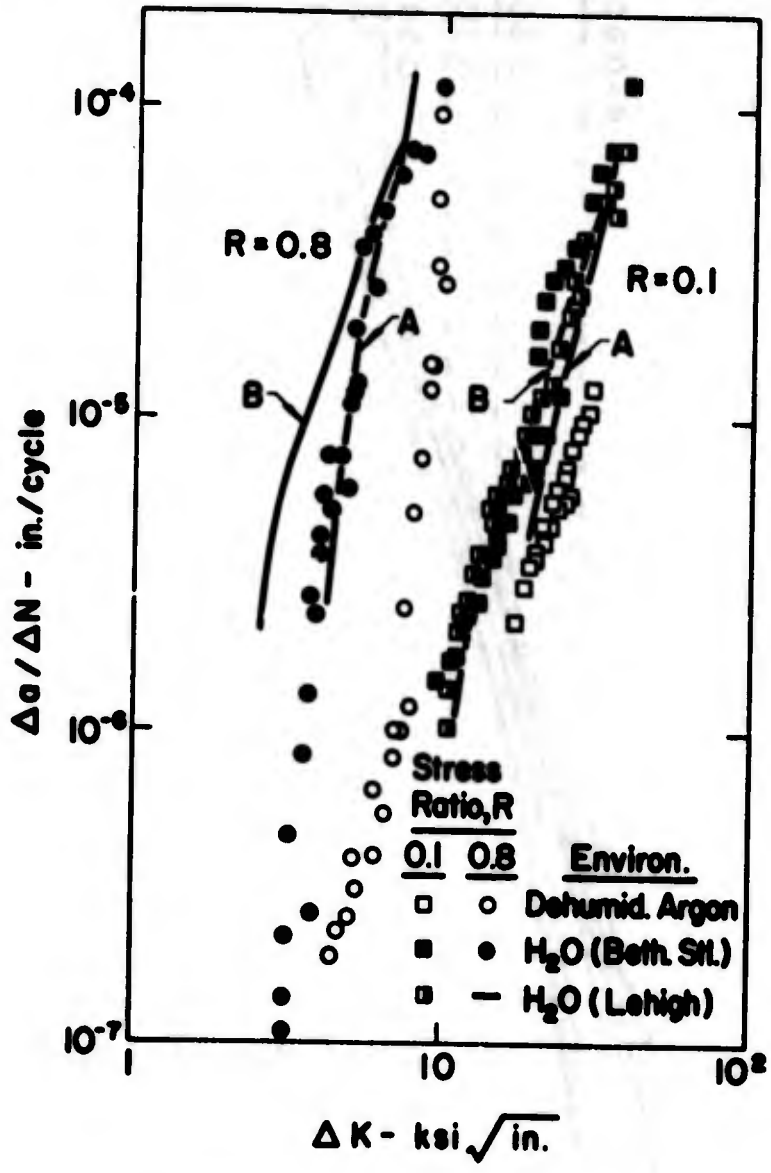

Figure 9: The Effect of Stress Ratio on Fatigue Crack Growth Kinetics (above K_{Iscc}) for AISI 4340 Steel Tempered at 200°F, f = 5.0 Hz [17].

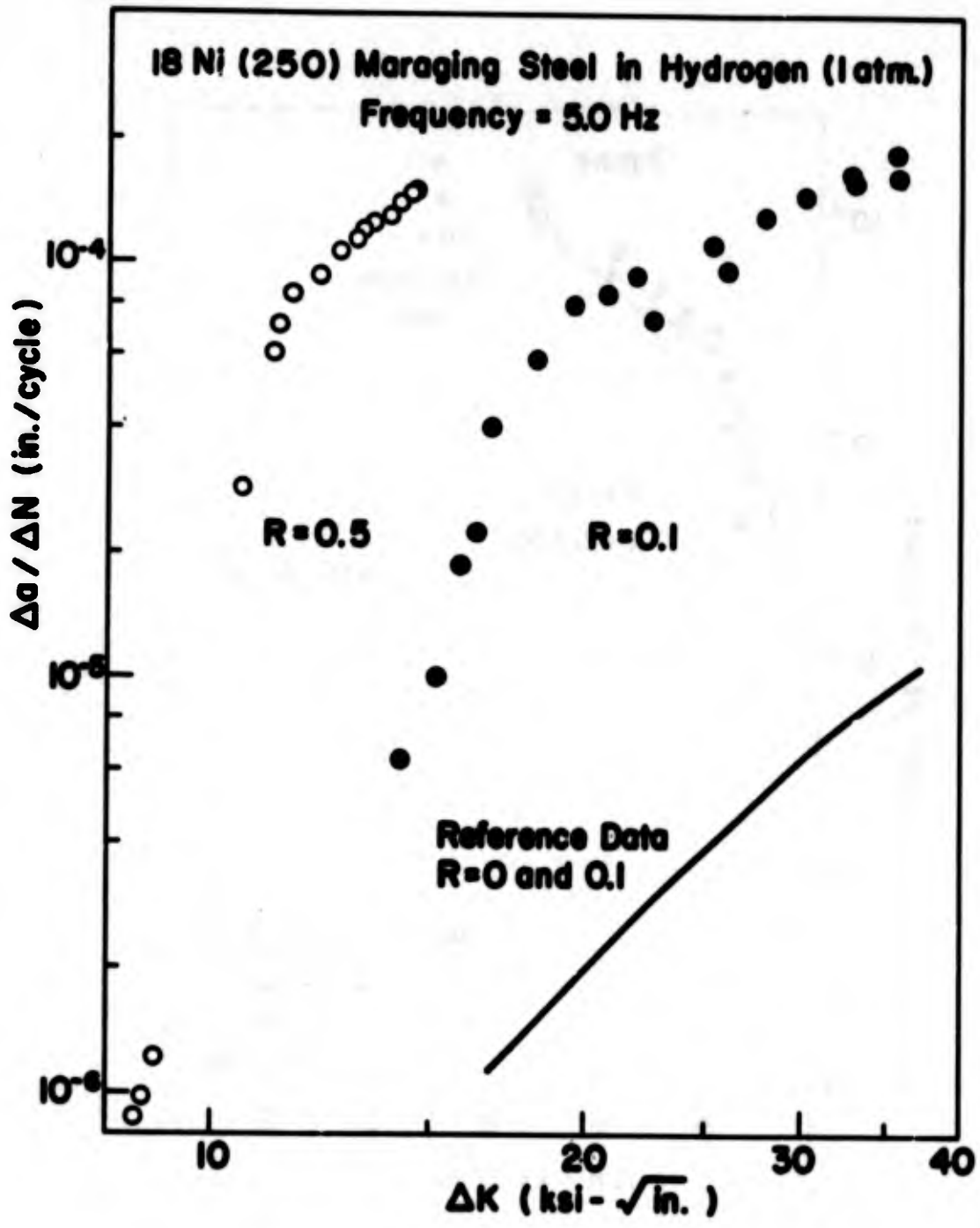

Figure 10: The Effect of Stress Ratio on Fatigue Crack Growth Kinetics (above K_{Iscc}) for 18Ni(250) Maraging Steel.

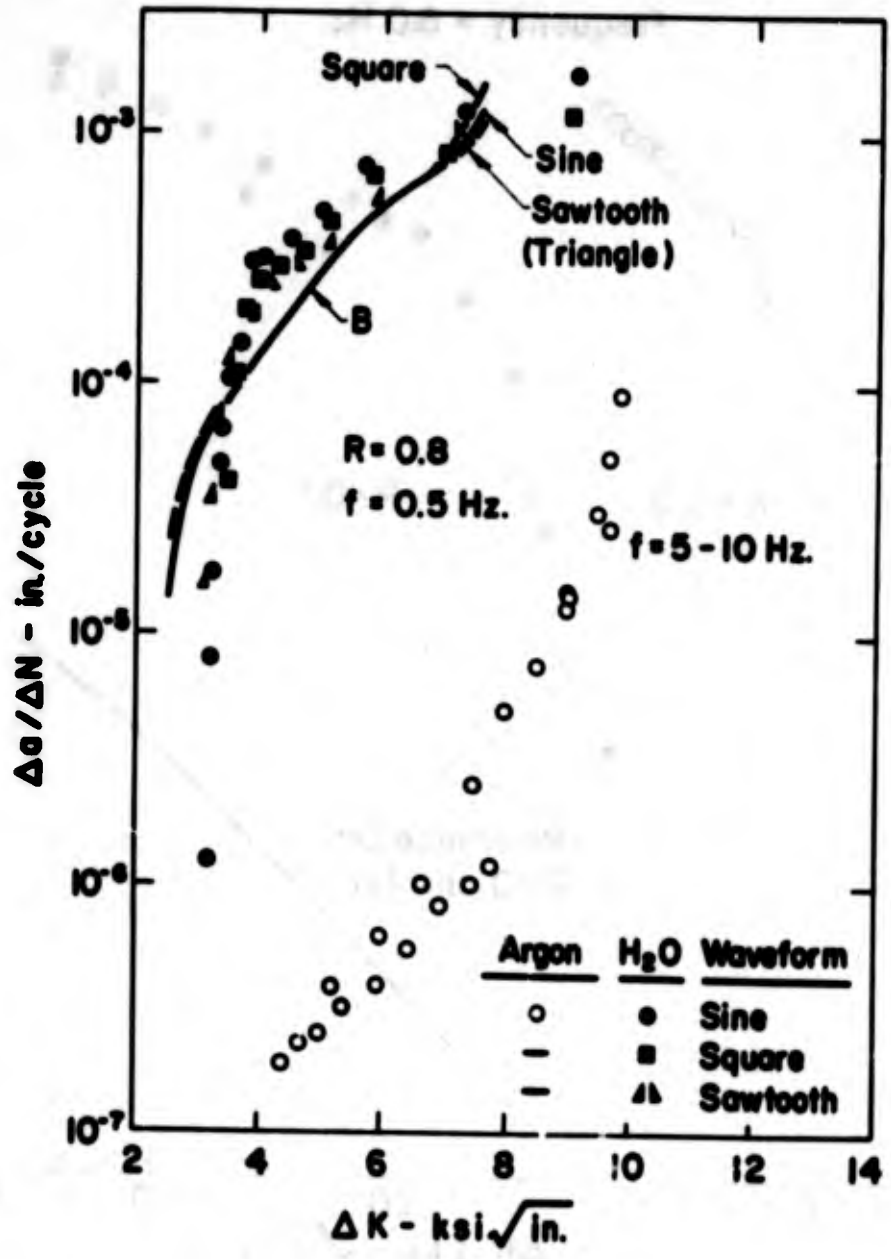

Figure 11(a): The Effect of Cyclic-Load Waveform on Fatigue Crack Growth (above K_{Iscc}) in AISI 4340 Steel Tempered at 200°F, R = 0.8. (Solid Lines Represent Predictions by the Wei-Landes Model [13]) [17].

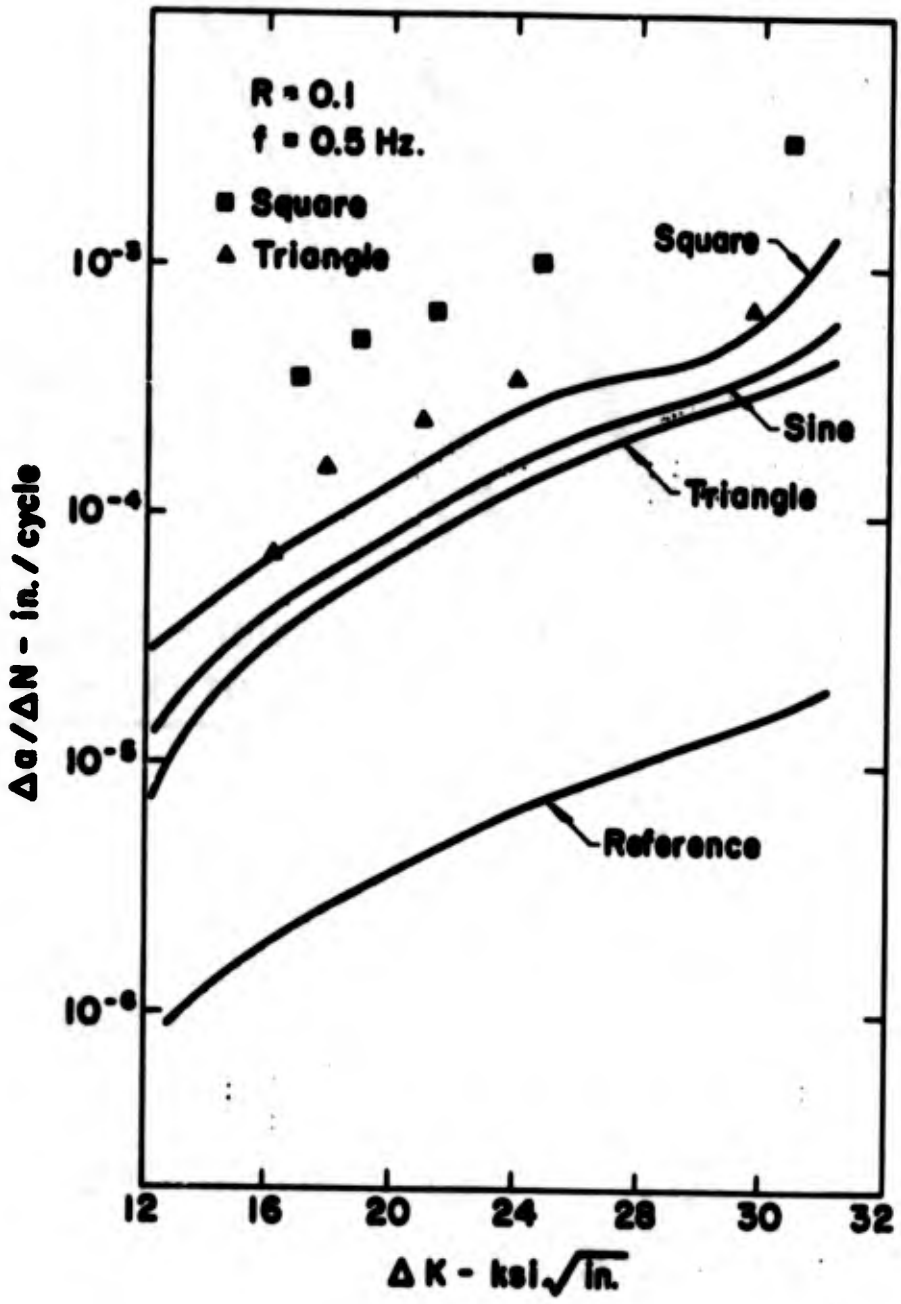

Figure 11(b): The Effect of Cyclic-Load Waveform on Fatigue Crack Growth (above K_{Iscc}) in AISI 4340 Steel Tempered at 200°F, R = 0.1. (Solid Lines Represent Predictions by the Wei-Landes Model [13]) [17].

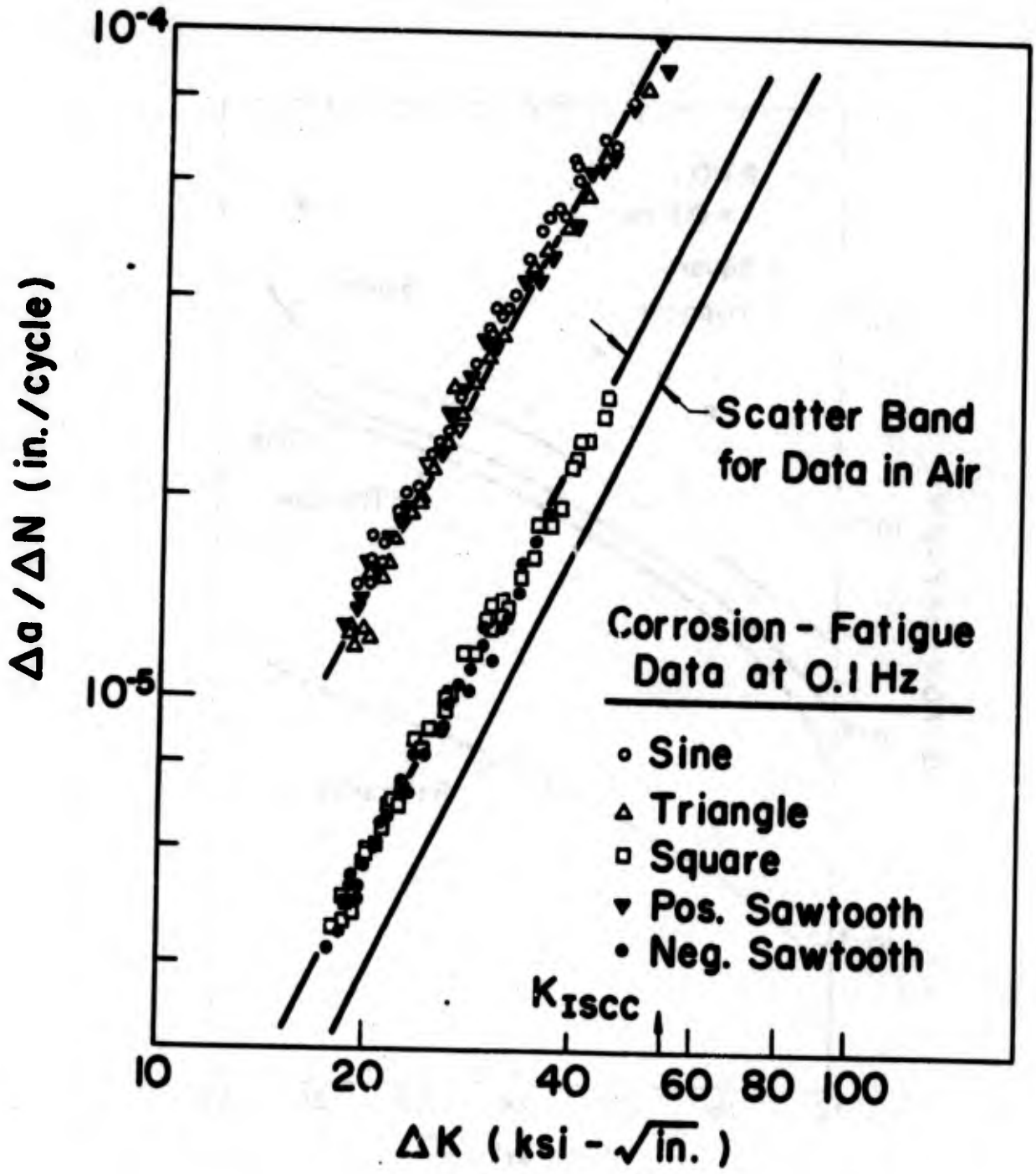

Figure 12: The Effect of Cyclic-Load Waveform on Fatigue Crack Growth (below K_{Iscc}) in 12Ni-5Cr-3Mo Steel, R = 0.25 [4].

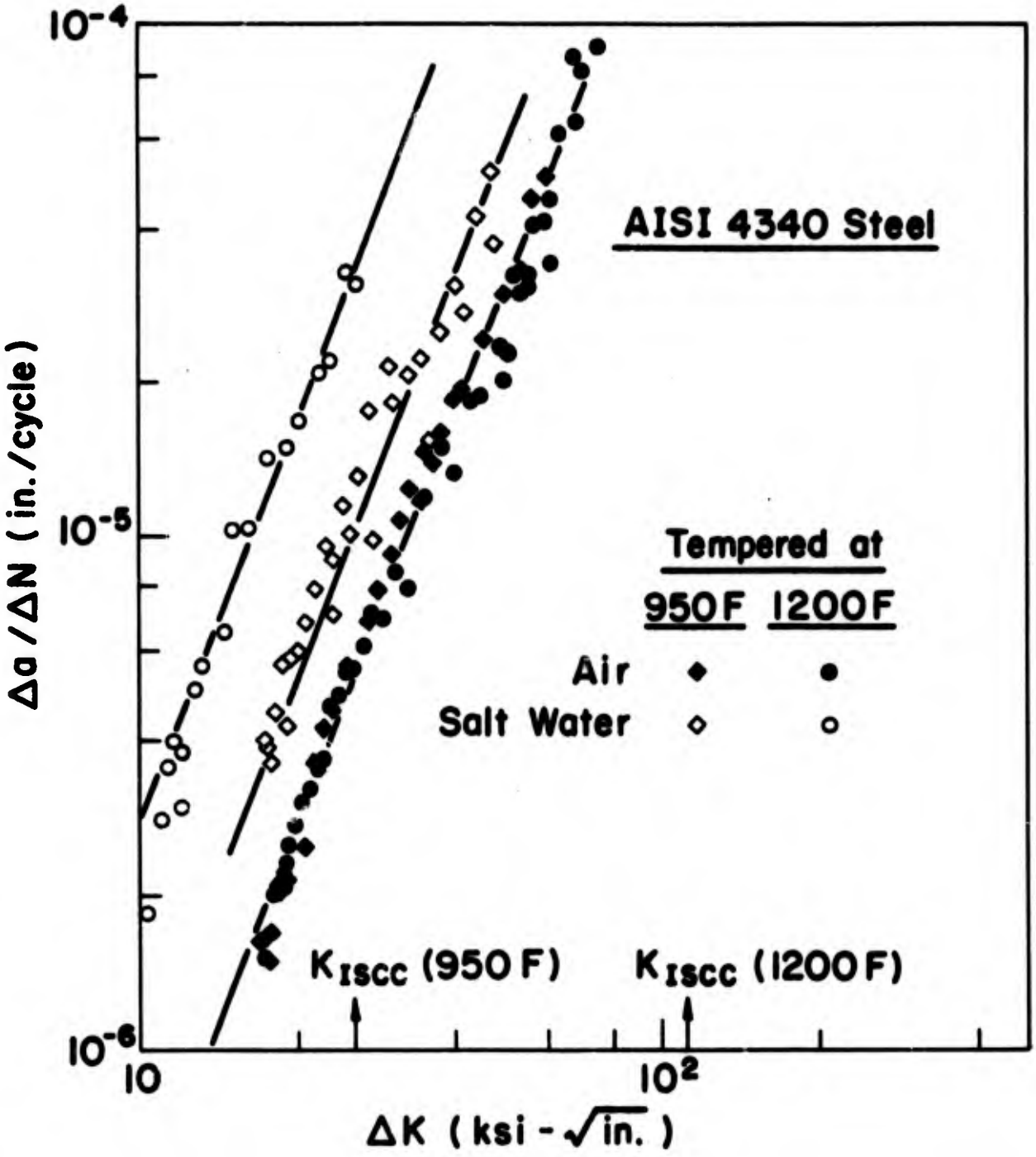

Figure 13: The Effect of Tempering Treatment on Fatigue Crack Growth in AISI 4340 Steel, $R \approx 0.1$ [28].

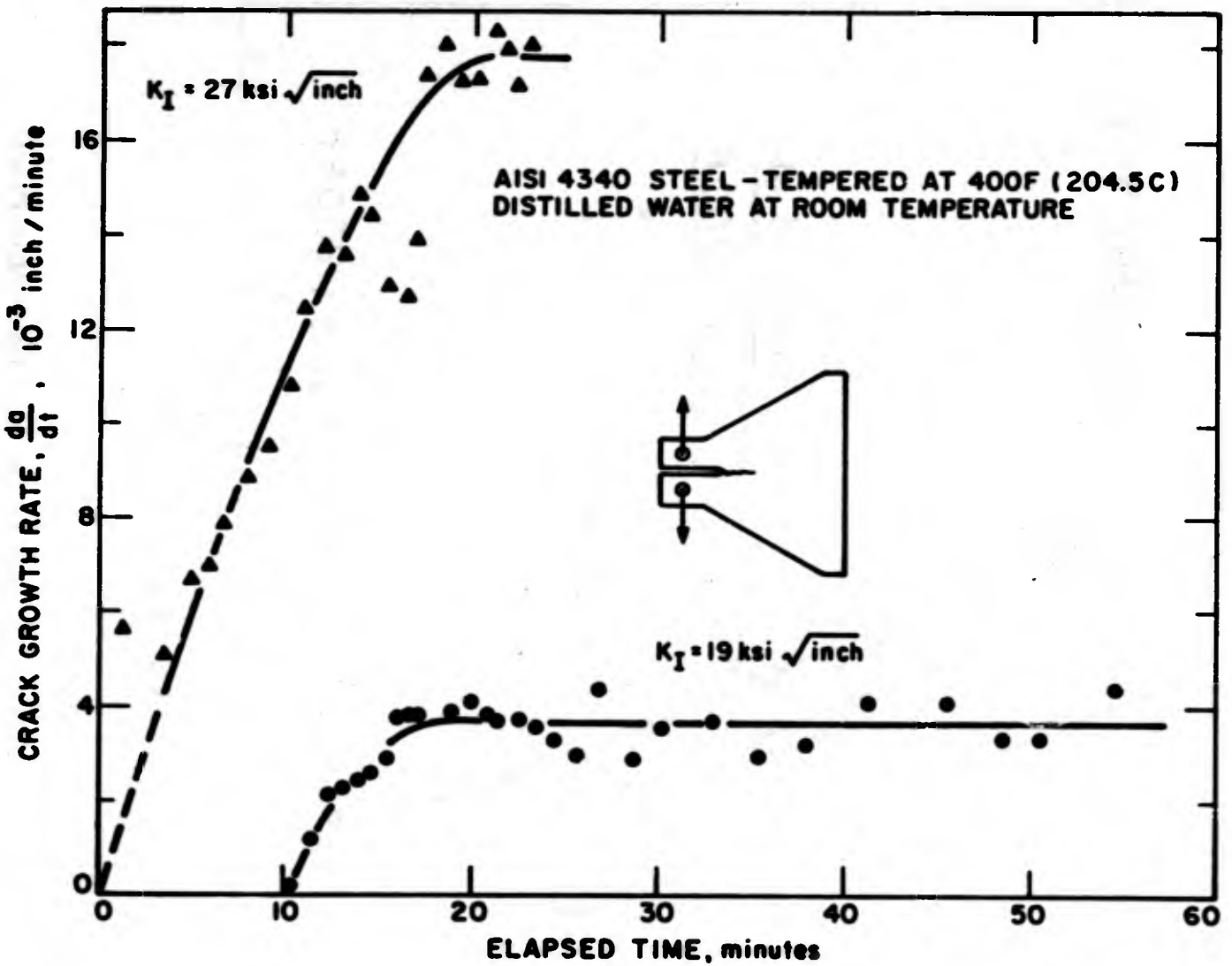

Figure 14: Sustained-Load Crack Growth under Constant K_I Showing Incubation, Crack Acceleration and Steady-State Stages of Crack Growth [11].

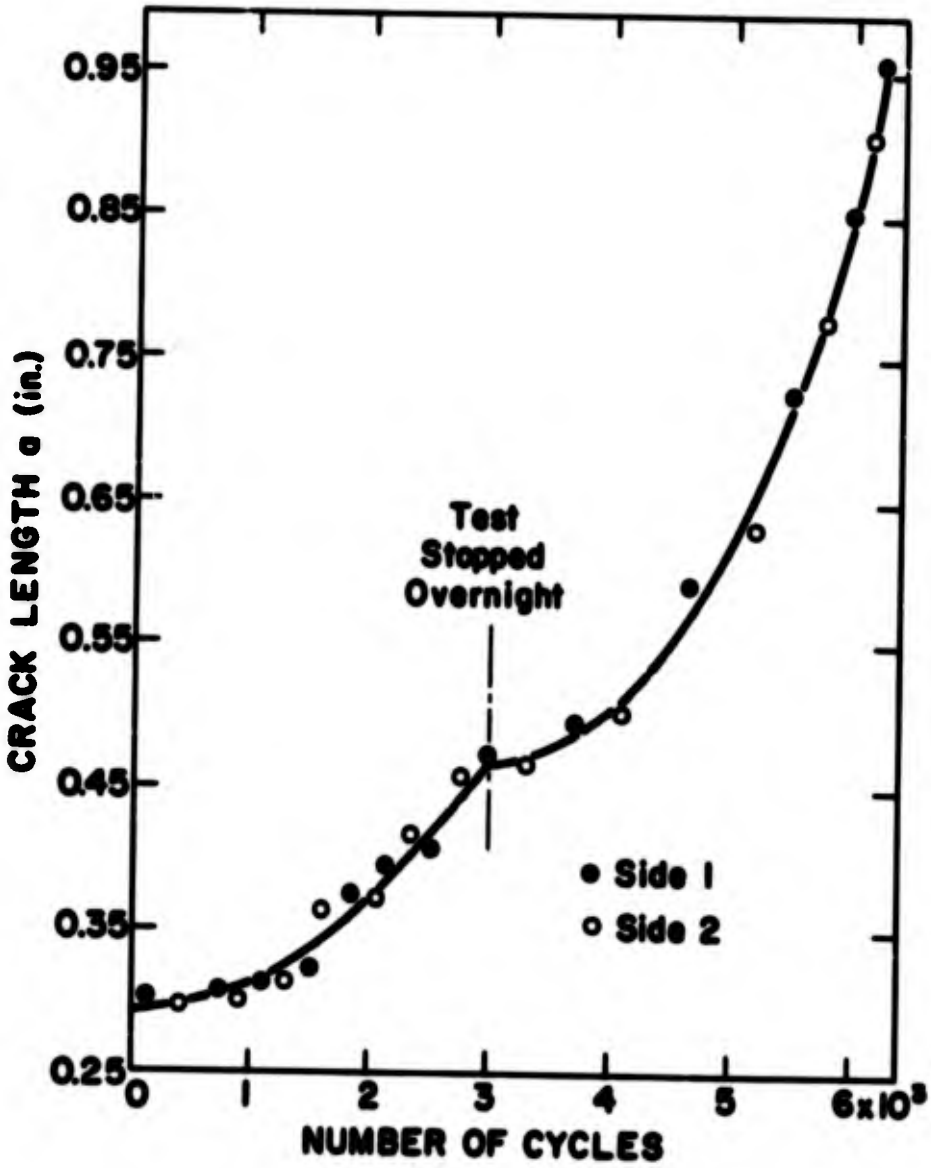

Figure 15: Fatigue Crack Growth Curve, for Constant-Amplitude Loading, Showing Nonsteady-State Behavior [17].

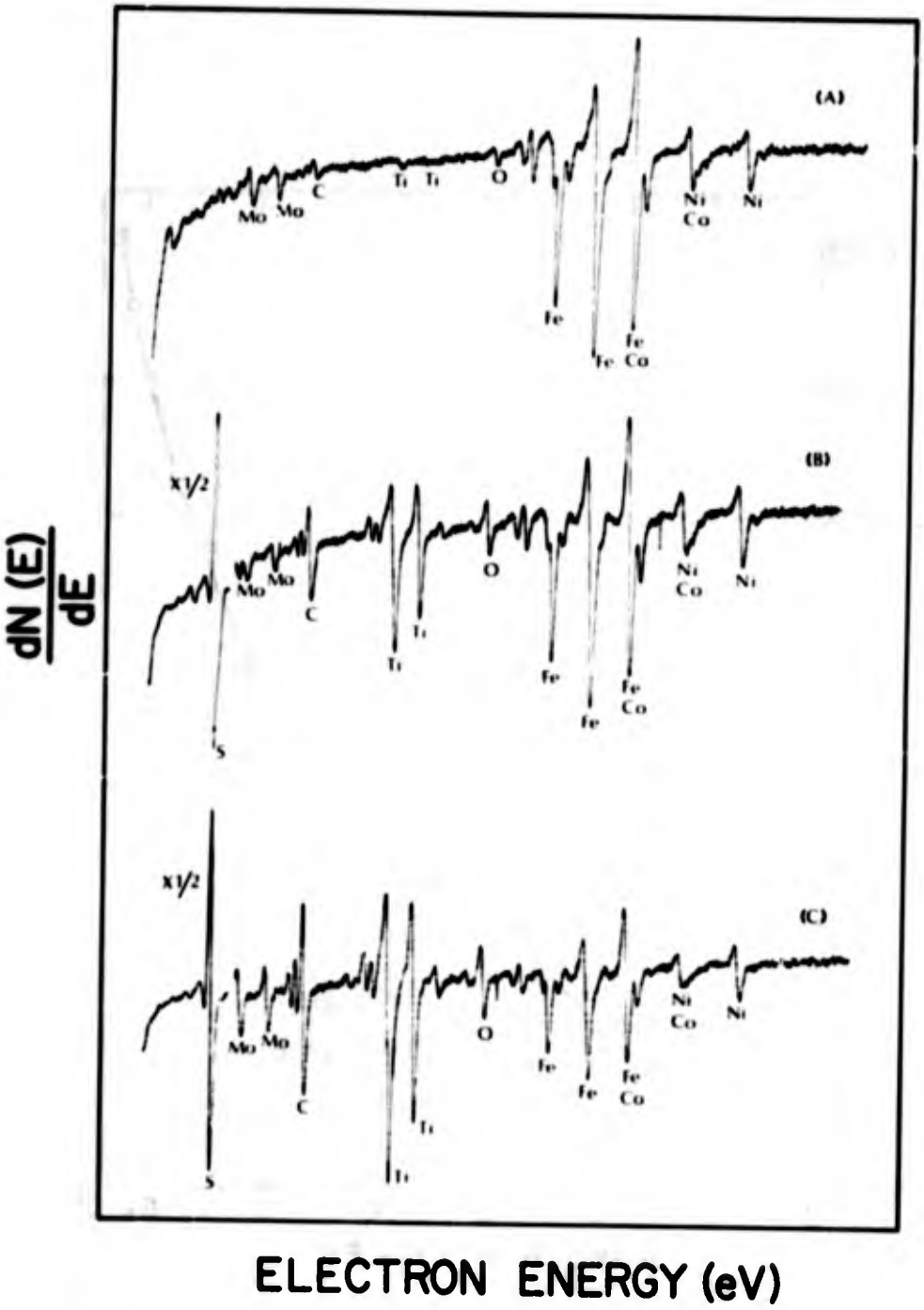

Figure 16: Auger Spectra of 18Ni(250) Maraging Steel, (A) "clean" surface, (B) after solution anneal, and (C) after aging.

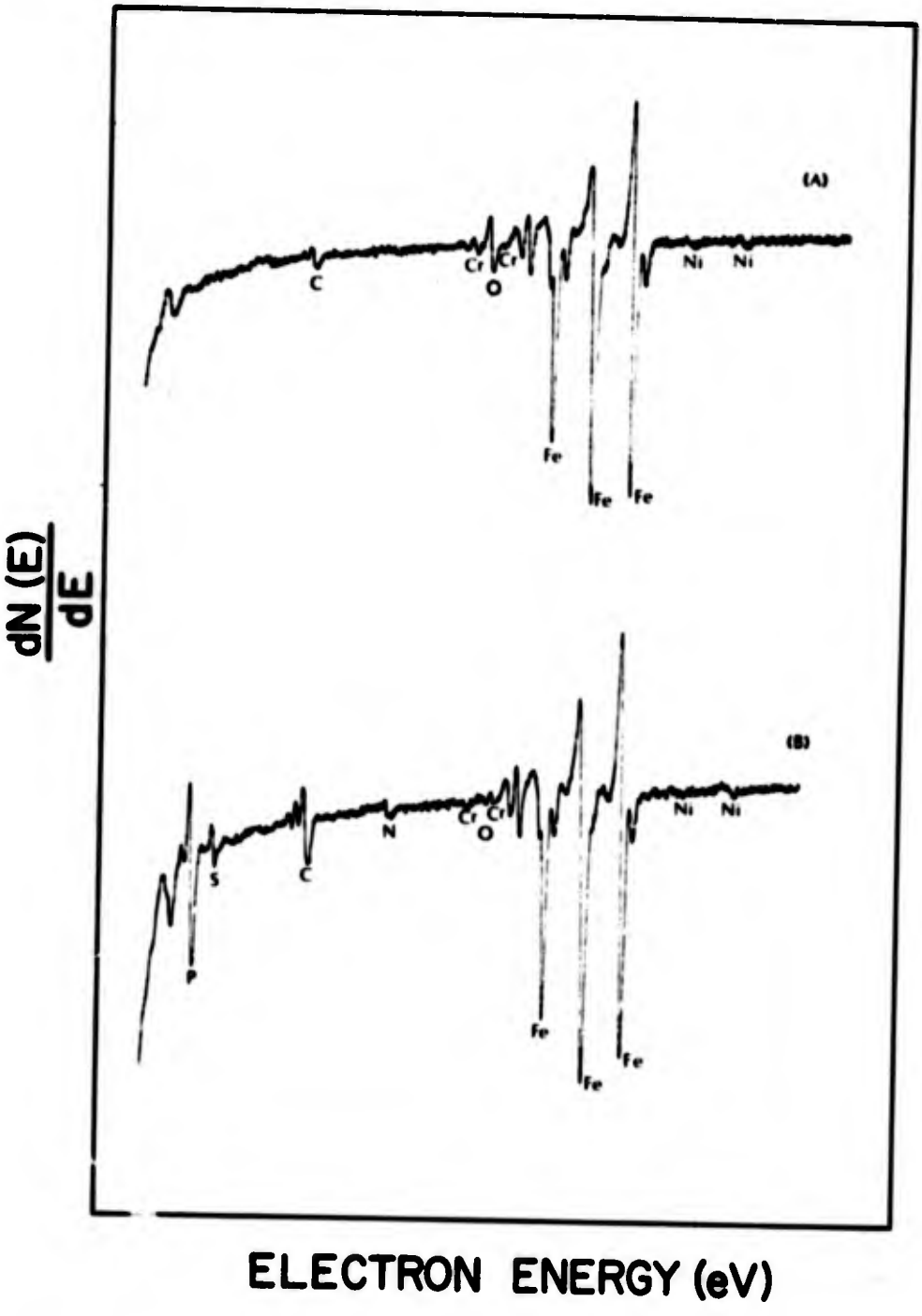

Figure 17: Auger Spectra of AISI 4340 Steel, (A) "clean" surface, (B) after austenitizing and tempering.

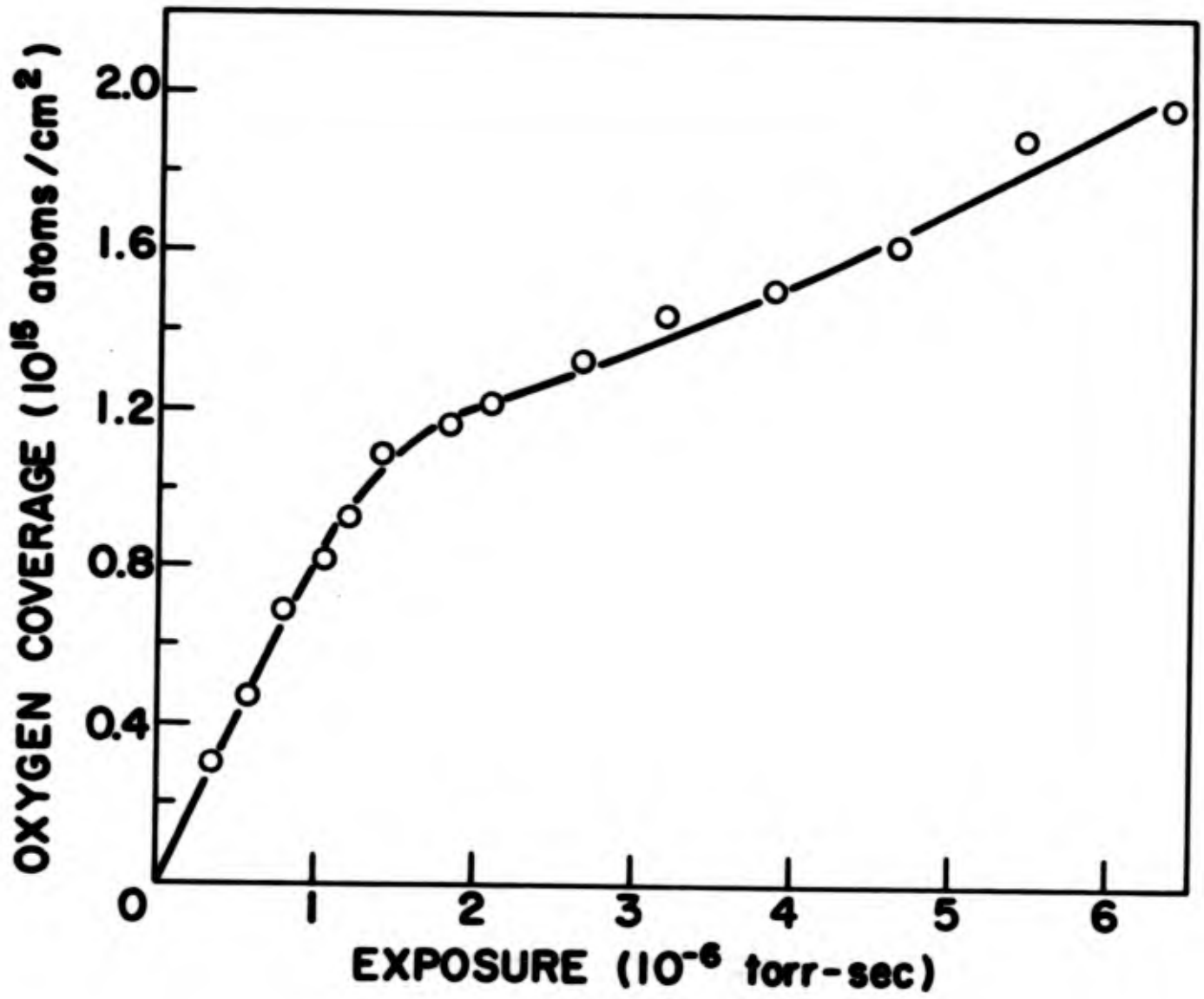

Figure 18: Initial Adsorption of Oxygen on Fe(001) at Room Temperature.

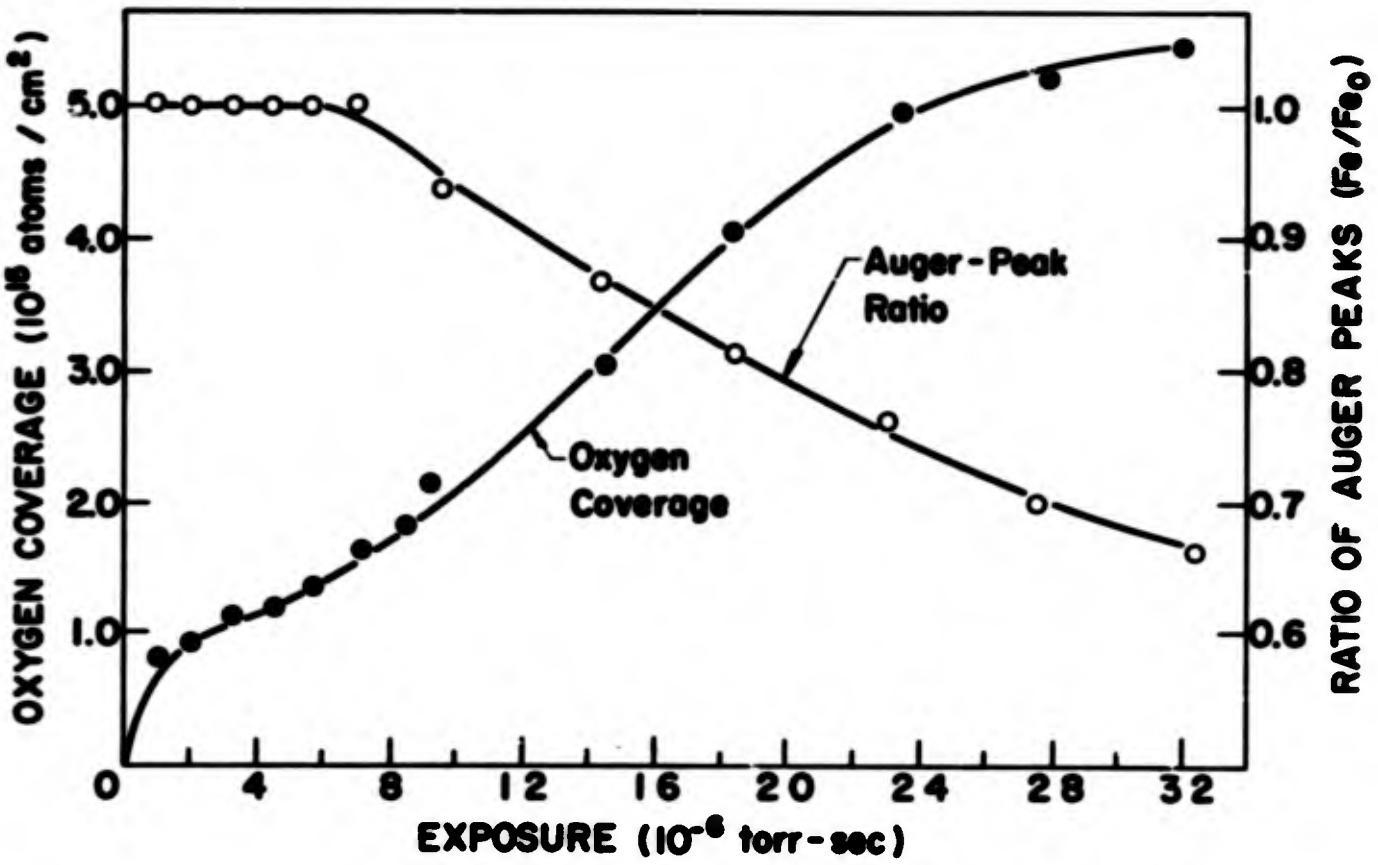

Figure 19: Oxygen Coverage and (Fe/Fe_0) as a Function of Exposure for Fe(001) at Room Temperature.

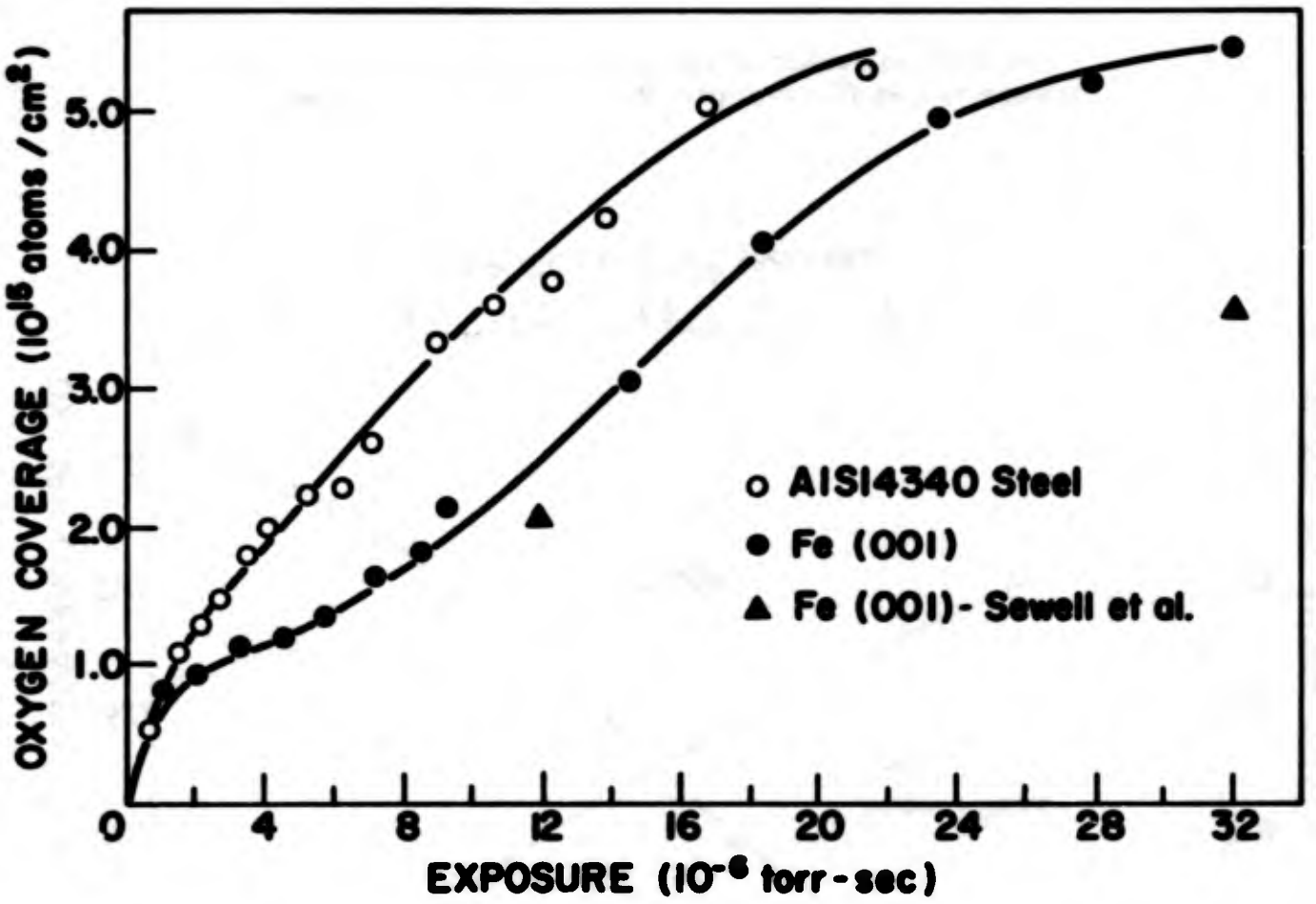

Figure 20: Adsorption of Oxygen on AISI 4340 Steel and Fe(001) at Room Temperature.